HEALTH AND MEDICINE

Stem cell–homing hydrogel-based miR-29b-5p delivery promotes cartilage regeneration by suppressing senescence in an osteoarthritis rat model

Jinjin Zhu[1,2]†, Shuhui Yang[2]†, Yadong Qi[3], Zhe Gong[1], Haitao Zhang[1], Kaiyu Liang[1], Panyang Shen[1], Yin-Yuan Huang[2], Zhe Zhang[2], Weilong Ye[2], Lei Yue[3], Shunwu Fan[1], Shuying Shen[1], Antonios G. Mikos[4], Xiumei Wang[2]*, Xiangqian Fang[1]*

Osteoarthritis (OA) is a common joint disease characterized by progressive loss of cartilage and reduction in lubricating synovial fluid, which lacks effective treatments currently. Here, we propose a hydrogel-based miRNA delivery strategy to rejuvenate impaired cartilage by creating a regenerative microenvironment to mitigate chondrocyte senescence that mainly contributes to cartilage breakdown during OA development. An aging-related miRNA, miR-29b-5p, was first found to be markedly down-regulated in OA cartilage, and their up-regulation suppressed the expression of matrix metalloproteinases and senescence-associated genes (*P16^{INK4a}*/*P21*) via ten-eleven-translocation enzyme 1 (TET1). An injectable bioactive self-assembling peptide nanofiber hydrogel was applied to deliver agomir-29b-5p, which was functionalized by conjugating a stem cell–homing peptide SKPPGTSS for endogenous synovial stem cell recruitment simultaneously. Sustained miR-29b-5p delivery and recruitment of synovial stem cells and their subsequent differentiation into chondrocytes led to successful cartilage repair and chondrocyte rejuvenation. This strategy enables miRNA-based therapeutic modality to become a viable alternative for surgery in OA treatment.

INTRODUCTION

Osteoarthritis (OA), the most common form of arthritis, is primarily characterized by the progressive loss of cartilage matrix and pathological changes in other joint components, such as osteophyte formation and synovial inflammation. By 2030, more than 67 million people are estimated to be afflicted with OA, with the total treatment costs exceeding $3 billion annually. Therefore, OA represents an enormous health and economic burden (*1*, *2*). Current standard of care for OA includes pain amelioration and eventual total joint replacement; the former is limited to relieving symptoms and improving joint function, and the latter is associated with infection and other comorbidities (*3*). However, there are no effective disease-modifying treatments that could prevent or suppress OA development.

The pathogenesis of OA is generally associated with aging and aberrant mechanical stress-induced changes in the chondrocyte microenvironment (*4*). The articular cartilage is a highly differentiated tissue that lacks blood vessels for nutrition supply, leading to a limited capacity for intrinsic repair. Thus, the preservation of robust chondrocytes in cartilage is paramount to joint health. Chondrocytes maintain cartilage homeostasis by synthesizing extracellular matrix (ECM), thus preserving the structural and functional integrity of the cartilage. However, in response to aging and aberrant mechanical stress stimuli, chondrocytes lose their ability to maintain cartilage integrity and their survival. Furthermore, they converse to catabolic cells that secrete matrix-degrading enzymes, such as matrix metalloproteinases (MMPs) and a disintegrin and metalloproteinase with thrombospondin motifs (ADAMTSs), including essential catabolic MMP13 and ADAMTS5 (*5*, *6*). These detrimental matrix changes further lead to both reduced mechanical integrity and diminished lubrication of cartilage, with subsequent accelerated cartilage wear and destruction (*7*). These OA risk factors lead to the cellular senescence of chondrocytes, a critical cellular event contributing to matrix metabolism imbalance during OA development (*8*). Thus, improving the local microenvironment and treating aging fundamentally will be promising strategies for treating OA.

Several key microRNAs (miRNAs) that target OA-associated genes, such as those of matrix-degrading enzymes, proinflammatory cytokines, and senescence, have been identified to play a crucial role in directing gene silencing in OA (*9*, *10*). The miR-29b, a member of the miR-29 family, is critically involved in chondrogenesis and OA, among which miR-29b-3p has been widely reported (*11*–*13*). Here, we therefore proposed to identify and deliver a previously unidentified senescence-associated miR-29b-5p for attenuating OA progression. However, the poor stability in vitro and in vivo, nonspecific distribution, and off-target effects of miRNA limit the use of therapeutic miRNA in the clinical setting (*14*, *15*). To improve the therapeutic efficiency of miRNAs, various vectors such as viruses, liposomes, cationic polymers, extracellular vesicles, and engineered exosomes have been developed for miRNA delivery (*16*, *17*). However, the biological toxicity, cellular immunoreactivity, and tumorigenicity of viral vectors limit their in vivo application (*18*). Nonviral vectors have attracted more attention because of their easy synthesis, low immune response, good biocompatibility, and improved safety (*19*). Particularly, agomir, a cholesterol-modified

[1]Department of Orthopedic Surgery, Sir Run Run Shaw Hospital, Zhejiang University School of Medicine and Key Laboratory of Musculoskeletal System Degeneration and Regeneration Translational Research of Zhejiang, Hangzhou 310016, China. [2]State Key Laboratory of New Ceramics and Fine Processing, Key Laboratory of Advanced Materials of Ministry of Education, School of Materials Science and Engineering, Tsinghua University, Beijing 100084, China. [3]Department of Gastroenterology, Sir Run Run Shaw Hospital, School of Medicine, Zhejiang University, Hangzhou 310016, Zhejiang Province, China. [4]Department of Bioengineering, Rice University, 6100 Main Street, Houston, TX 77005, USA.
*Corresponding author. Email: orthofxq@zju.edu.cn (X.F.); wxm@mail.tsinghua.edu.cn (X.W.)
†These authors contributed equally to this work.

miRNA mimic, can form micelles and is efficiently internalized by cells, resulting in improved cartilage degeneration (*10*).

In addition to inhibiting cellular senescence, rejuvenation of the joint as a whole and further to promote cartilage repair is necessary to counteract progressive cartilage breakdown during OA by recruitment of stem cells to differentiate into new young chondrocytes. Because of a very close embryologic link between the cartilage and the synovium, synovium-derived mesenchymal stem cells (SMSCs) have been demonstrated to improve cartilage repair (*20*, *21*). However, considering the large size of human knee joints, SMSCs are unlikely to migrate over long distances to reach the site of injuries. Previously, we designed a self-assembling peptide (SAP) that was functionalized with a bone marrow–homing peptide (BMHP) motif, SKPPGTSS, to modulate MSC homing (*22*, *23*). This functional peptide promotes cartilage defect repair after microfracture (MF), and it might have the same effect on SMSCs.

Liquid therapeutics alone cannot improve the lubrication properties of synovial fluid when the levels of hyaluronic acid in osteoarthritic joints are low, which usually leads to increased wear and tear of the cartilage surfaces (*24*). Therefore, injectable hydrogels with favorable lubricating properties are preferable to protect the joints and relieve pain while repairing cartilage defects. Macroscopic biopolymer hydrogels, such as alginate and collagen, have been reported to provide localized and sustained delivery of small interfering RNA (siRNA) (*25*). Here, we propose a novel strategy to generate a regenerative intra-articular microenvironment by delivering an aging-related miR-29b-5p using a stem cell–homing hydrogel, which inhibits the abnormal metabolism of cartilage matrix and promotes the repair of cartilage defects by recruiting synovium-derived stem cells. Self-assembly of synthetic peptides can yield an array of well-defined nanostructures, which are highly attractive nanomaterials for many biomedical applications such as drug delivery (*26*). In the physiological environment, the SAP, Ac-$(RADA)_4$-NH_2 (RADARADARADARADA-NH_2) can self-assemble and undergo gelation into a hydrogel with good biocompatibility and excellent mechanical properties (*27*). The hydrogel has a porous structure that mimics the natural ECM, thereby serving as a promising medium for drug release and cell delivery (*28*). Furthermore, various functional peptide epitopes can be easily integrated with the self-assembling backbones to achieve specific functions for the precise treatment of various diseases (*29*).

In this study, a miRNA (miR-29b-5p) was verified to inhibit the senescence and anabolism/catabolism imbalance of chondrocytes, which silenced the downstream ten-eleven-translocation enzyme 1 (*TET1*) gene. Next, the agomir-29b-5p was integrated into functionalized SAPs containing the stem cell–homing sequence SKPPGTSS to form an injectable hydrogel (SKP@miR). Last, we evaluated its treatment effect on cartilage defect and recruitment of SMSCs in an anterior cruciate ligament transection (ACLT) rat model.

RESULTS

Identification of miR-29b-5p on alleviating chondrocyte senescence and attenuating OA progression via TET1

We first identified a previously unknown senescence-associated miRNA in chondrocytes linked to OA progression. The physiological niches from which chondrocytes are isolated are at low-oxygen tensions. Primary chondrocytes exposed to prolonged normoxia exhibited senescence phenotypes with up-regulated $P16^{INK4a}$ (*30*). Thus, we performed miRNA sequencing in chondrocytes undergoing serial passaging under normoxia and identified several miRNAs that were differentially down-regulated with the onset of senescence (fig. S1A). These down-regulated miRNAs were compared with the down-regulated miRNAs of OA [GSE (gene expression omnibus series) 48266] and aged cartilage (GSE 105027), followed by species conservation analysis in humans, rats, and mice, resulting in nine miRNAs that regulated both senescence and OA. Further experimental screening revealed that miR-29b-5p, among the nine miRNAs, was significantly down-regulated in both senescent chondrocytes and interleukin-1β (IL-1β)–induced OA chondrocytes from humans and rats (fig. S1, B to E).

To further explore the association between miR-29b-5p and OA pathogenesis, we evaluated the expression of cartilage ECM (*Col2a1* and *Aggrecan*), necessary transcription factor *Sox9*, degradative enzymes (*Mmp3*, *Mmp13*, *Adamts4*, and *Adamts5*), and senescent-related indicators ($P16^{INK4a}$ and *P21*) involved in OA pathogenesis (*31*, *32*). According to Western blot (WB) and quantitative real-time polymerase chain reaction (qRT-PCR) results, miR-29b-5p overexpression up-regulated the expression of *Col2a1*, *Aggrecan*, and *Sox9* but down-regulated the expression of *Adamts4*, *Adamts5*, *Mmp3*, *Mmp13*, $P16^{INK4a}$, and *P21* (Fig. 1, A and B). In an aged mouse model of knee OA, the sustained overexpression of miR-29b-5p led to thicker cartilage and down-regulated MMP13 and P21 (cyclin-dependent kinase inhibitor 1A) (Fig. 1C). The fluorescence in situ hybridization (FISH) in chondrocytes revealed that the miR-29b-5p was predominantly localized in the cytoplasm (Fig. 1D). These results suggest that miR-29b-5p is a kind of protective miRNA in cytoplasm, which would alleviate OA by overexpression to induce a decline in catabolic enzymes and senescence-related genes and a rise in cartilage ECM synthesis.

To further demonstrate that miR-29b-5p was up-regulated at the molecular level to control the senescence and OA processes, we performed RNA sequencing to profile the transcriptome of chondrocytes transfected with agomir-NC (negative control) and agomir-29b-5p (Fig. 1E). Hierarchical clustering was conducted to sort differentially down-regulated genes based on their coexpression patterns to determine the functional modules, which are the sets of genes implicated in a biological process and controlled by miR-29b-5p (*33*). This clustering revealed four distinct gene sets enriched with sequence-based miR-29b-5p targets, reflecting the functional modules inactivated by miR-29b-5p down-regulation (fig. S2, A and B). Pathway analysis indicated that the identified gene sets were associated with annotations related to "PI3K-Akt," "Rap1," "Ras," or "ECM-receptor" (fig. S2, C and D). The representative genes involved in cellular senescence and OA exhibited interrelated network, with corresponding changes in gene expression (fig. S2E) (*34*).

Among the four functional gene modules, clusters 2 and 3 were the most highly enriched with the predicted miR-29b-5p targets and were strongly associated with terms related to cellular senescence and OA. Next, we used miRWalk and TargetScan, in combination with the sequencing results, to predict genes that are directly regulated downstream. *TET1*, one of the targets, is a relatively important gene in senescence and OA, and the functions of TET1 are in concert in humans and rats (*35*, *36*). Agomir-29b-5p reduced the TET1 expression (Fig. 1, F and G), whereas antagomir-29b-5p exerted opposite effects as evidenced by WB and qPCR results (Fig. 1, H and I). Furthermore, the miR-29b-5p significantly inhibited luciferase activity in cells transfected with double wild-type 3′ untranslated region (3′UTR) of *Tet1* but not in those with its mutant (Fig. 1J). *Tet1*

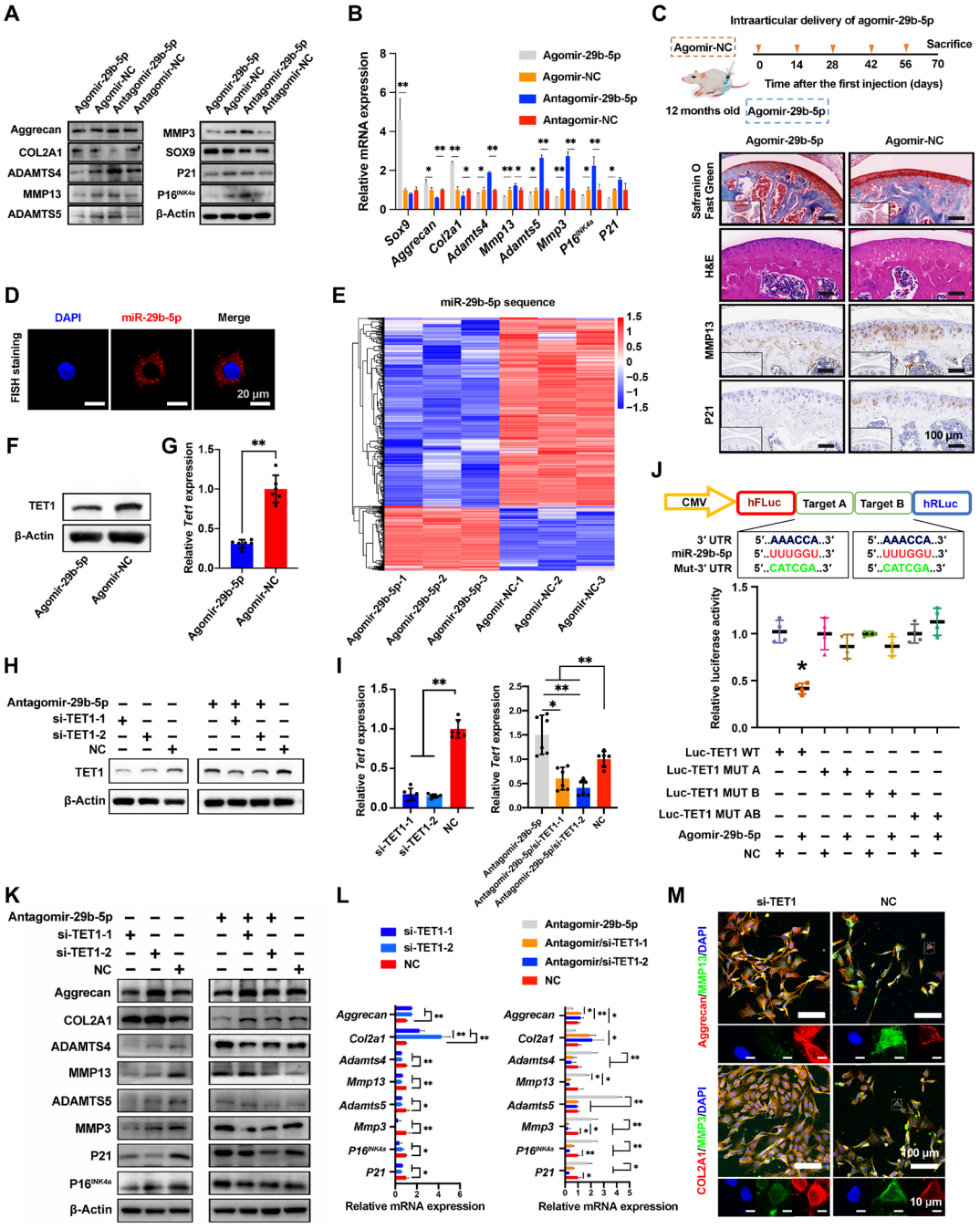

Fig. 1. Identification of functions and targets of miR-29b-5p. (**A** and **B**) Expression of COL2A1, aggrecan, SOX9, MMP3, MMP13, ADAMTS4, ADAMTS5, P16^{INK4a}, and P21 at 2 days after transfection of agomir-29b-5p, agomir-NC, antagomir-29b-5p, and antagomir-NC to rat chondrocytes determined by WB (A) and qRT-PCR (B) ($n = 4$). (**C**) Schematic illustration of agomir-29b-5p delivery schedules in aging mice. Representative images of knee cartilage stained with Safranin O/Fast Green and hematoxylin and eosin (H&E) and immunostained with MMP13 and P21. $n = 5$ mice per group. (**D**) FISH analysis of miR-29b-5p in rat chondrocytes. (**E**) Sequencing results of rat chondrocytes transfected with agomir-29b-5p and agomir-NC. $n = 3$. (**F** to **I**) TET1 expression at 2 days after transfection of agomir-29b-5p (F and G), si-TET1, and/or antagomir-29b-5p (H and I) to rat chondrocytes determined by WB (F and H) and qRT-PCR (G and I) ($n = 6$). (**J**) Luciferase reporter assay of *Tet1* in human embryonic kidney (HEK) 293T cells after transfection with agomir-29b-5p or NC. $n = 4$. (**K** and **L**) Expression of COL2A1, aggrecan, MMP3, MMP13, ADAMTS4, ADAMTS5, P16^{INK4a}, and P21 at 2 days after transfection of si-TET1 and/or antagomir-29b-5p to rat chondrocytes determined by WB (K) and qRT-PCR (L) ($n = 4$). (**M**) Immunofluorescence staining of rat chondrocytes at 2 days after si-TET1 transfection. Data are presented as means ± SD. Statistical analysis was performed using two-tailed Student's *t* test for (B) and (G) and one-way analysis of variance (ANOVA) for (I), (J), and (L). *$P < 0.05$ and **$P < 0.01$. DAPI, 4′,6-diamidino-2-phenylindole.

knockdown also decreased the expression of *Mmp3*, *Mmp13*, *Adamts4*, *Adamts5*, *P16*^{INK4a}, and *P21* but increased the expression of *Aggrecan* and *Col2a1* (Fig. 1, K to M). In addition, TET1 and miR-29b-5p acted antagonistically to each other, while miR-29b-5p exhibited more robust function. Therefore, it is concluded that miR-29b-5p is involved in the regulation of OA progression through multiple senescence-related signaling pathways, including TET1 inhibition.

Sustained delivery of miR-29b-5p from SKP@miR system

The delivery of agomir-29b-5p offered a promising strategy to treat OA via postponing chondrocyte senescence and protecting against decreased cartilage matrix production. However, the stability of agomirs can only be maintained for 1 week, and repeated injection is time-consuming and impractical. To overcome this challenge, we engineered an SAP hydrogel-based delivery system to prolong the retention of agomir-29b-5p in the knee joint (Fig. 2A). Particularly, a cationic functional peptide SKPPGTSS was introduced into the hydrogel for more sustained and stable release and for endogenous stem cell recruitment. Under macroscopic observation, precipitation was not observed upon mixing agomir-29b-5p and the peptide solutions. After equilibration with phosphate-buffered saline (PBS), the SAPs gelled into a homogeneous hydrogel and appeared transparent, suggesting the uniform distribution of agomirs and the injectable capacity into joint cavity to form hydrogels in the humoral environment (Fig. 2B). The characteristic peak at 840 cm^{-1} in the Fourier transform infrared (FTIR) spectra of RAD@miR and SKP@miR, reflecting the phosphate and sugar vibrations in agomirs, indicated the existence of agomir-29b-5p in the composite hydrogels (fig. S3A). Besides, the integration of agomirs had no effect on the β sheet structure and nanofiber formation of SAPs (fig. S3, B and C).

The agomir-29b-5p was mainly integrated with the repeated RADA sequence of RAD peptide via hydrogen bonds and electrostatic interactions (Fig. 2C and fig. S3, D and E). With the involvement of SKP peptide, the agomirs tended to combine with the functional motif sequence SKPPGTSS instead of RADA sequence because of the positively charged lysine. Compared to RAD peptides with a ZRank score at −45, the SKP peptide had stronger binding affinity to agomir-29b-5p, suggested by a lower score at −50 (fig. S3, F and G). Although arginine in RAD sequences was also positively charged, it would participate in self-assembly process and combine with aspartic acid, which competed with the integration of agomirs. Fluorescein isothiocyanate (FITC)–labeled agomirs were uniformly distributed and retained in RAD@miR and SKP@miR because of the interaction of agomirs and peptides (Fig. 2D and fig. S4, A and B). These results suggested stronger binding between agomir-29b-5p and SKP, contributing to permanent release.

All hydrogels exhibited a nanofibrous network structure, with pores ranging from 50 to 200 nm, contributing to maintaining agomirs and offering a profitable three-dimensional microenvironment for cell growth (Fig. 2E and fig. S4, C and D) (*37*). In a relatively stable environment in vitro, agomirs in SKP@miR were released relatively slowly to about 70% in 40 days, not as markedly as those in RAD@miR with an abrupt release in only 10 days (Fig. 2F). To evaluate the retention of agomir-29b-5p in vivo, RAD@miR and SKP@miR labeled with Cy5.5 (Cyanine5.5) were injected into the knee joints at 7 days after ACLT and monitored via a live imaging system (Fig. 2G). The encapsulated agomirs were retained in the joints for up to 14 days in both groups, and the fluorescence signal in the joints injected with SKP@miR was much higher than those injected with RAD@miR at 5, 7, 9, and 14 days, indicating the better retention of agomirs in SKP@miR (fig. S4E).

To evaluate the uptake of agomir-29b-5p by SMSCs and rat chondrocytes, agomirs labeled with FITC were used for cell culture. Compared with tissue culture plate, where the agomirs were only taken up by a small fraction of cells, SKP@miR and RAD@miR promoted the extensive and uniform uptake of agomirs, without affecting the adhesion and viability of cells (Fig. 3A and fig. S4F). To study the penetration of agomirs in cartilage, agomir-29b-5p was labeled with Cy5.5, and porcine cartilage explants were incubated with RAD@miR and SKP@miR and pure agomir solution for 5 days. The released agomirs accumulated at the cartilage surface at day 1 and gradually penetrated inside the cartilage by approximately 200 μm by day 5 in both SKP@miR and RAD@miR groups (Fig. 3B). Quantitative analysis of the fluorescence images revealed that the penetration depth of agomirs in hydrogels was significantly lower than that of pure agomir solution at day 1; however, the penetration depth of agomirs in SKP@miR reached a comparable level to that of pure agomir solution at day 5, indicating the sustained release of agomir-29b-5p (fig. S5A). To verify the in vivo effect of released agomir-29b-5p on OA, we injected SKP@miR into rat knee joints at 4 weeks after ACLT. At 7 and 10 weeks after ACLT, FISH of harvested joints revealed a persistently higher level of miR-29b-5p expression in the joints in SKP@miR group than that in the other groups, indicating that the release of agomir-29b-5p from SKP@miR might contribute to an extended effect on attenuating OA (Fig. 3C). Together, these results demonstrated that SKP@miR could provide ECM-mimicking structure and long-term sustained release of biologically active agomir-29b-5p capable of being taken up by cells without cytotoxicity.

SKP@miR rescues OA cartilage degeneration after ACLT surgery

The therapeutic effect of SKP@miR on OA after being injected into rat knee joints at 4 weeks after ACLT was evaluated. Joint effusion, inflammation, periarticular osteophyte formation, and adhesions were not observed in the SKP@miR group. Micro–computed tomography (micro-CT) scans showed increased osteophyte production, indicating unbalanced bone reconstruction. The knee joints in the SKP@miR group had few osteophytes, which were comparable to the normal joints, whereas osteophytes were clearly seen in the PBS, miR, and SKP groups (Fig. 4A). There were partial fractures, defects, and osteoporosis in the subchondral bone in the case of early OA, which was improved in the late stage. Particularly, the subchondral bone in the SKP@miR group was more stable and almost comparable to that in the sham group (fig. S5, B to E). Synovitis is another sign of OA (*38*, *39*). The total synovitis scores in knees in the SKP@miR group at 7 and 10 weeks were comparable to those in the sham group, significantly lower than those in the PBS, miR, and SKP groups. The thickening of the synovial lining layer was significantly relieved with SKP@miR relative to PBS (Fig. 4, B and C, and fig. S5, F to H).

On the basis of hematoxylin and eosin (H&E) and Safranin O/Fast Green staining, knee joints in the SKP@miR group maintained cartilage integrity and displayed minor signs of degeneration at 7 and 10 weeks (Fig. 4D). Histological scoring that grades the microscopic structure of the repair cartilage revealed obvious improvements in cell morphology, matrix staining, and cartilage appearance in the SKP@miR group, which was comparable to that in the sham group

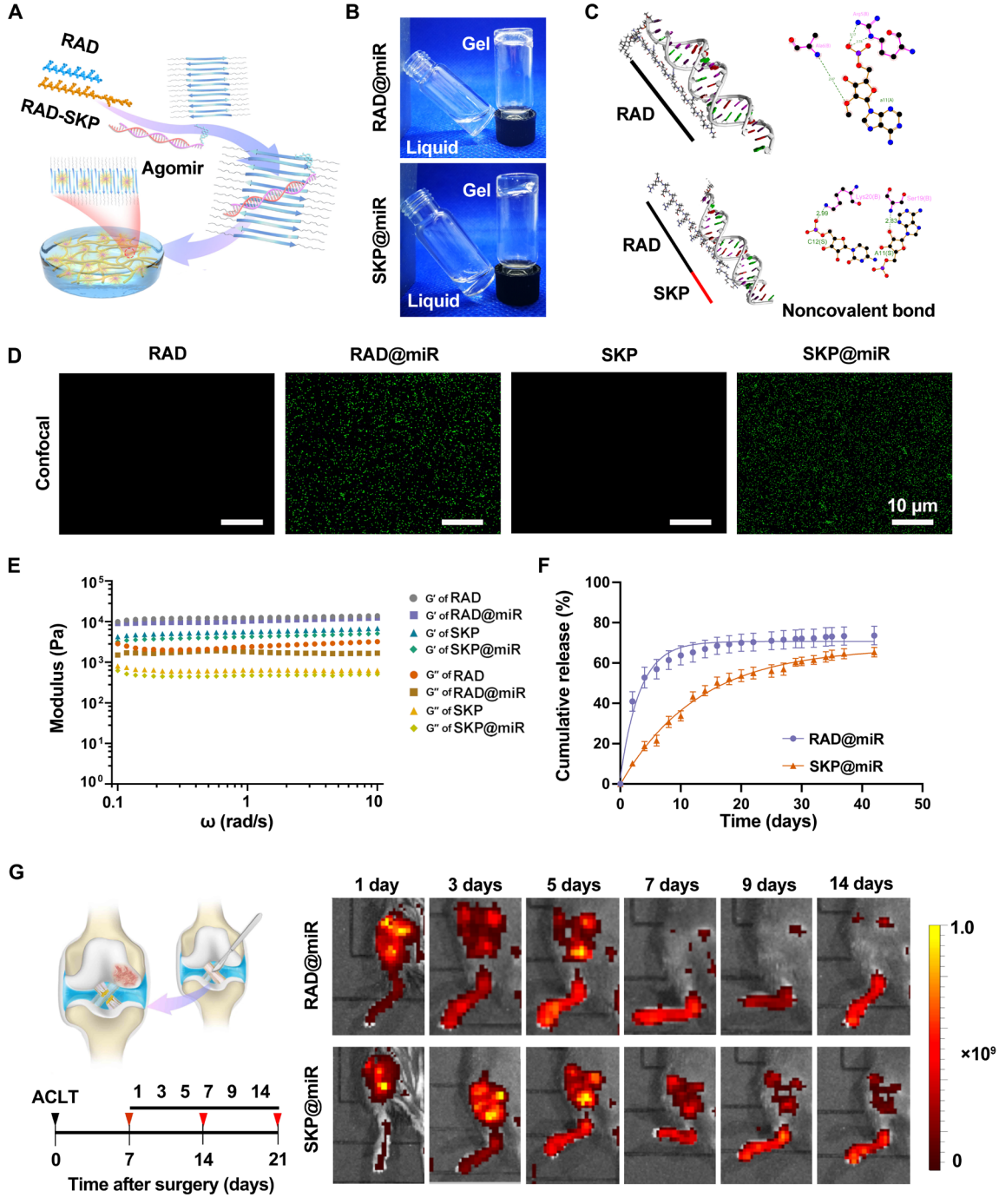

Fig. 2. Characterization of hydrogel-based miR-29b-5p delivery system. (**A**) Schematic illustration of SKP@miR. RAD and SKP peptides self-assemble to form a nanofiber hydrogel with agomir-29b-5p distributed inside. (**B**) RAD and SKP peptides with agomir-29b-5p form stable hydrogels by adjusting the pH value to neutral. (**C**) Molecular docking analysis of RAD or SKP peptide interacted with agomir-29b-5p. (**D**) FITC-labeled agomir-29b-5p in RAD, RAD@miR, SKP, and SKP@miR. (**E**) Rheological measurements of storage (G′) and loss (G″) moduli of RAD, RAD@miR, SKP, and SKP@miR (0.1 to 10 rad/s at 0.5% strain). (**F**) Cumulative release of agomir-29b-5p in RAD@miR and SKP@miR in a 37°C incubator. $n = 3$. (**G**) Schematic illustration of ACLT-induced OA model and in vivo imaging of Cy5.5-labeled agomir-29b-5p in mice joints at 1, 3, 5, 7, 9, and 14 days after intra-articular injection of hydrogels. Color represents radiant efficiency [(p s^{-1} cm^{-2} sr^{-1})/(μW cm^{-2})]. $n = 3$ mice per group. Data are presented as means ± SD.

(Fig. 4E and fig. S5, I to M). Moreover, the Osteoarthritis Research Society International (OARSI) score was significantly lower in the SKP@miR group than that in the PBS, miR, and SKP groups, without significant difference compared with sham group (Fig. 4F). It is also noted that the OARSI score decreased at 10 weeks compared with that at 7 weeks in the SKP@miR group, indicating the improved cartilage repair over time, while the scores remained almost constant in the other groups. The hot plate reaction time was significantly shorter in the SKP@miR group than those in the PBS, miR, and SKP groups, indicating the relief of OA-induced pain (Fig. 4G). Therefore,

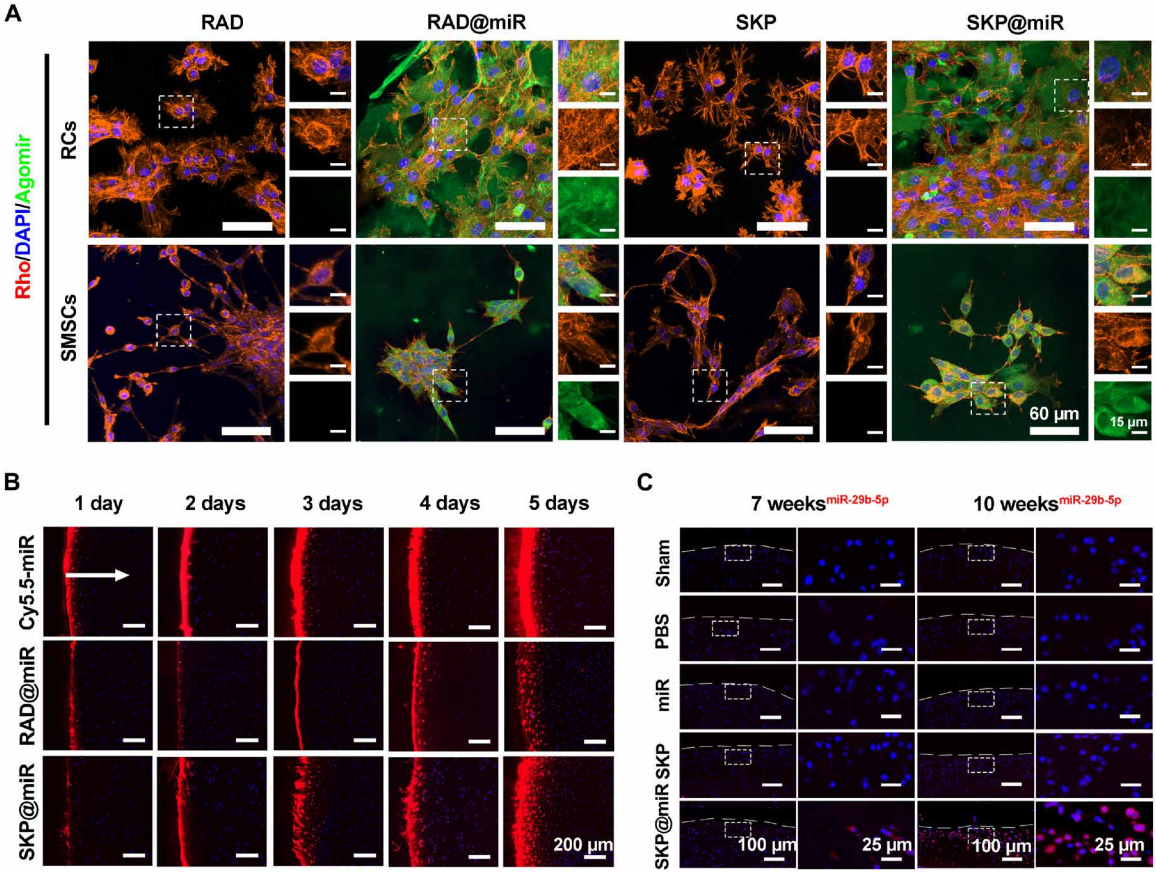

Fig. 3. Uptake and penetration of agomirs released from hydrogels in vitro and extended effect in vivo. (**A**) Representative confocal images of rat chondrocytes (RCs) and SMSCs after being cultured on RAD, RAD@miR, SKP, and SKP@miR for 2 days. Agomir-29b-5p were labeled with FITC. F-actin was stained with rhodamine phalloidin (Rho), and nuclei were stained with DAPI. (**B**) Representative confocal microscopy images of cross sections of porcine cartilage explants incubated with free Cy5.5-labeled agomir-29b-5p, RAD@miR, and SKP@miR for 1, 2, 3, 4, and 5 days. The arrow indicates the diffusion direction. (**C**) FISH analysis of miR-29b-5p in rat knee cartilage at 7 and 10 weeks after surgery. Nuclei were stained with DAPI in (B) and (C).

these results demonstrated a good therapeutic efficacy of intra-articular injection of SKP@miR on cartilage repair in OA.

SKP@miR alleviates senescence and maintains catabolic balance in cartilage

The senescence and catabolic balance in the cartilage was evaluated via immunohistochemical staining. A representative COL2A1 (collagen type II alpha 1 chain) up-regulation and a notable decrease in the levels of MMP13, $P16^{INK4a}$, and P21 in the SKP@miR group were observed at 7 weeks, approaching that in the sham group. At 10 weeks, the effect of SKP@miR group was comparable to that of the sham group (Fig. 5A). The quantitative analysis revealed that COL2A1-positive cells in SKP@miR group were significantly more than those in the control groups (PBS, miR, and SKP), while the TET1-, P21-, $P16^{INK4a}$-, or MMP13-positive cells were significantly less than those in the control groups, indicating decreased senescence and increased matrix synthesis (Fig. 5, B and C). In addition, the P21- and $P16^{INK4a}$-positive cells were further significantly decreased, while COL2A1-positive cells were significantly increased in the SKP@miR group at 10 weeks compared with those at 7 weeks, which was not observed in other groups, suggesting the enduring effect of agomir-29b-5p in SKP@miR.

To comprehensively elucidate the underlying mechanisms through which SKP@miR alleviates senescence, we validated the effect on chondrocytes in vitro. Primary chondrocytes on the hydrogels showed permanent vitality and good adhesion, indicating that the hydrogels were nontoxic and biocompatible (fig. S6, A and B). SKP@miR effectively alleviated chondrocyte senescence with a significantly decreased number of SA (senescence-associated)–β-galactosidase (β-Gal)–positive cells (Fig. 6, A and B). The toluidine blue and Alcian blue staining revealed that SKP@miR was more conducive to form chondrogenic matrix (Fig. 6C). Immunofluorescence results showed that SKP@miR promoted the expression of aggrecan and COL2A1 and inhibited the expression of MMP3, P21, and $P16^{INK4a}$ in chondrocytes (Fig. 6D).

To investigate the effect of SKP@miR on senescent chondrocytes, cells were induced to a senescent phenotype via incubation with doxorubicin and successive generations, respectively (*4*). Senescent cells were significantly decreased when cultured on SKP@miR (Fig. 6B and fig. S6, C and D). The proliferation and cell viability of senescent cells was promoted on SKP@miR compared with that on other hydrogels (fig. S6, E to G). Notably, the expression levels of $P16^{INK4a}$, *P21*, and *P53* in chondrocytes induced by doxorubicin were significantly down-regulated on SKP@miR compared with those on RAD, while only the expression of $P16^{INK4a}$ in P3 cells on RAD@miR and SKP@miR was lower than that on RAD and SKP, reflecting that the agomir-releasing hydrogels eliminated chondrocyte senescence caused by DNA damage (fig. S6, H to J).

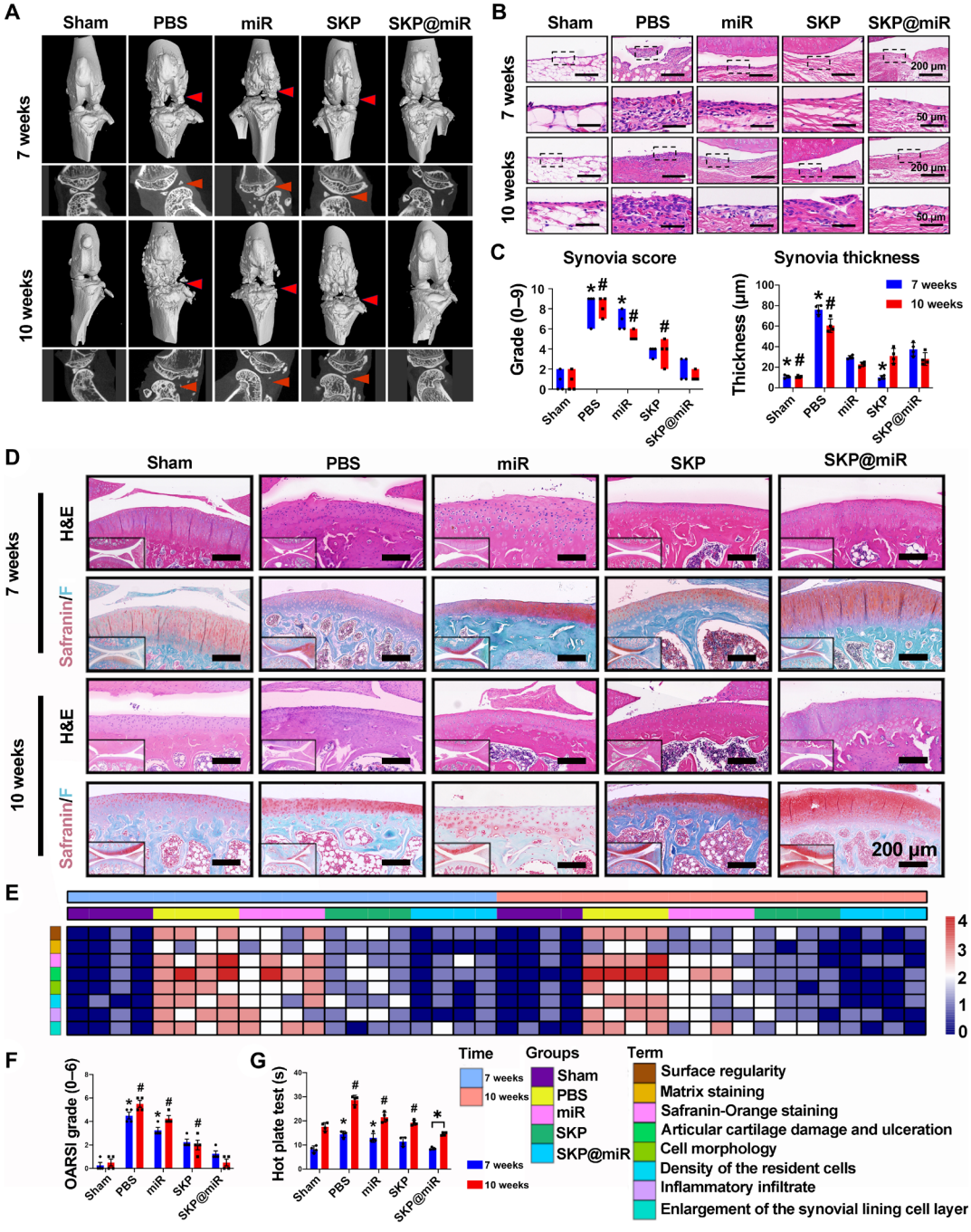

Fig. 4. SKP@miR rescues OA cartilage degeneration after ACLT surgery in rats. (**A**) Three-dimensional and planar view reconstruction images of rat knee joints showing the abnormal growth of osteophytes (indicated by arrow) in sham, PBS, miR, SKP, and SKP@miR groups at 7 and 10 weeks. (**B**) Morphological analysis of the synovium at 7 and 10 weeks indicated by H&E staining. (**C**) Synovia thickness and total synovia scores of enlargement of the synovial lining cell layer, inflammatory infiltrates, and density of the resident cells. (**D**) Representative rat knee joint images stained with Safranin O/Fast Green and H&E at 7 and 10 weeks. (**E**) Heatmap of variables of histological scoring at 7 and 10 weeks. **(F)** OARSI grades of rat joints at 7 and 10 weeks. (**G**) Hot plate test of rats at 7 and 10 weeks. $n = 4$ rats per group. Data are presented as means ± SD. Statistical analysis was performed using one-way ANOVA for intergroup comparison with SKP@miR at 7 or 10 weeks (*$P < 0.05$ versus SKP@miR group at 7 weeks and #$P < 0.05$ versus SKP@miR group at 10 weeks) and two-tailed Student's *t* test for comparing data at 7 and 10 weeks in SKP@miR group (*$P < 0.05$) in (C), (F), and (G).

To evaluate the therapeutic effects on OA from a cellular perspective, we constructed chondrocytes with OA phenotype by stimulating normal chondrocytes with IL-1β to simulate an in vivo chronic inflammatory environment (*31*). SKP@miR substantially up-regulated the expression of SOX9 (sex determining region Y-box transcription factor 9), aggrecan, and COL2A1 and down-regulated the expression of degradative enzymes in normal chondrocytes; however, after chondrocytes were induced to the arthritis phenotype with

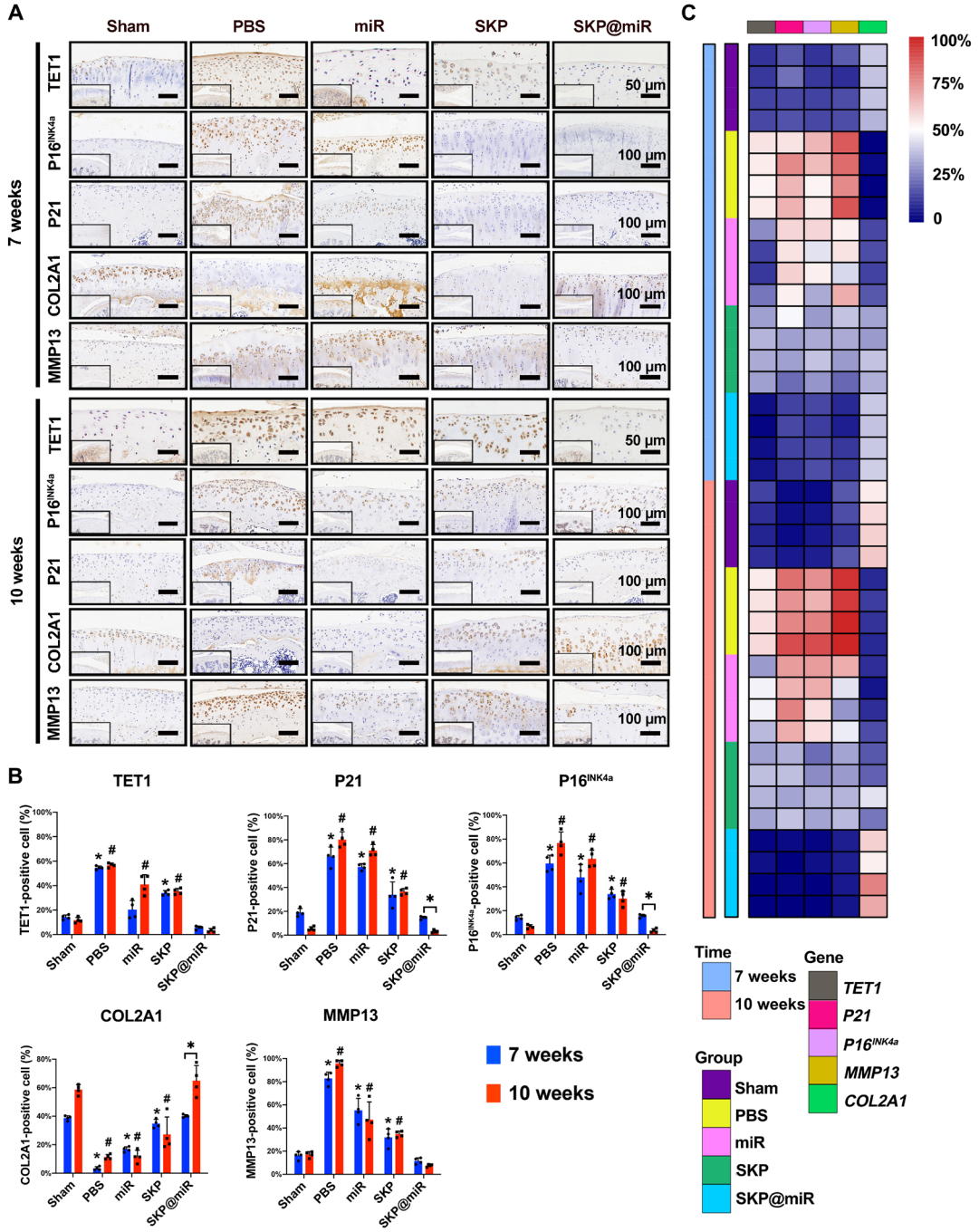

Fig. 5. SKP@miR effectively attenuates senescence of rat joints. (**A**) Representative immunohistochemistry staining images of TET1, P16^{INK4a}, P21, COL2A1, and MMP13 of rat knee joints from sham, PBS, miR, SKP, and SKP@miR groups at 7 and 10 weeks. (**B**) Quantification of histology positive cells of TET1, P21, P16^{INK4a}, COL2A1, and MMP13. (**C**) Heatmap of positive cell rate of TET1, P21, P16^{INK4a}, MMP13 and COL2A1. $n = 4$ rats per group. Data are presented as means ± SD. Statistical analysis was performed using one-way ANOVA for intergroup comparison with SKP@miR at 7 or 10 weeks (*$P < 0.05$ versus SKP@miR group at 7 weeks and #$P < 0.05$ versus SKP@miR group at 10 weeks) and two-tailed Student's *t* test for comparing data at 7 and 10 weeks in SKP@miR group (*$P < 0.05$) in (B).

IL-1β, the regulations on these factors were even more pronounced (Fig. 6, E and F, and fig. S7, A and B). Furthermore, the expression of TET1 in chondrocytes was down-regulated on SKP@miR (Fig. 6G). Therefore, SKP@miR could alleviate chondrocyte senescence and maintain catabolic balance in cartilage, contributing to attenuating OA progression.

SKP@miR induces recruitment and chondrogenic differentiation of SMSCs

Here, the SKP peptide was confirmed to have a positive effect on the recruitment of SMSCs from synovium to aid in the repair of damaged cartilage in OA (Fig. 7A). The joints were stained with CD90 and CD73, which were important markers for SMSCs. Note that

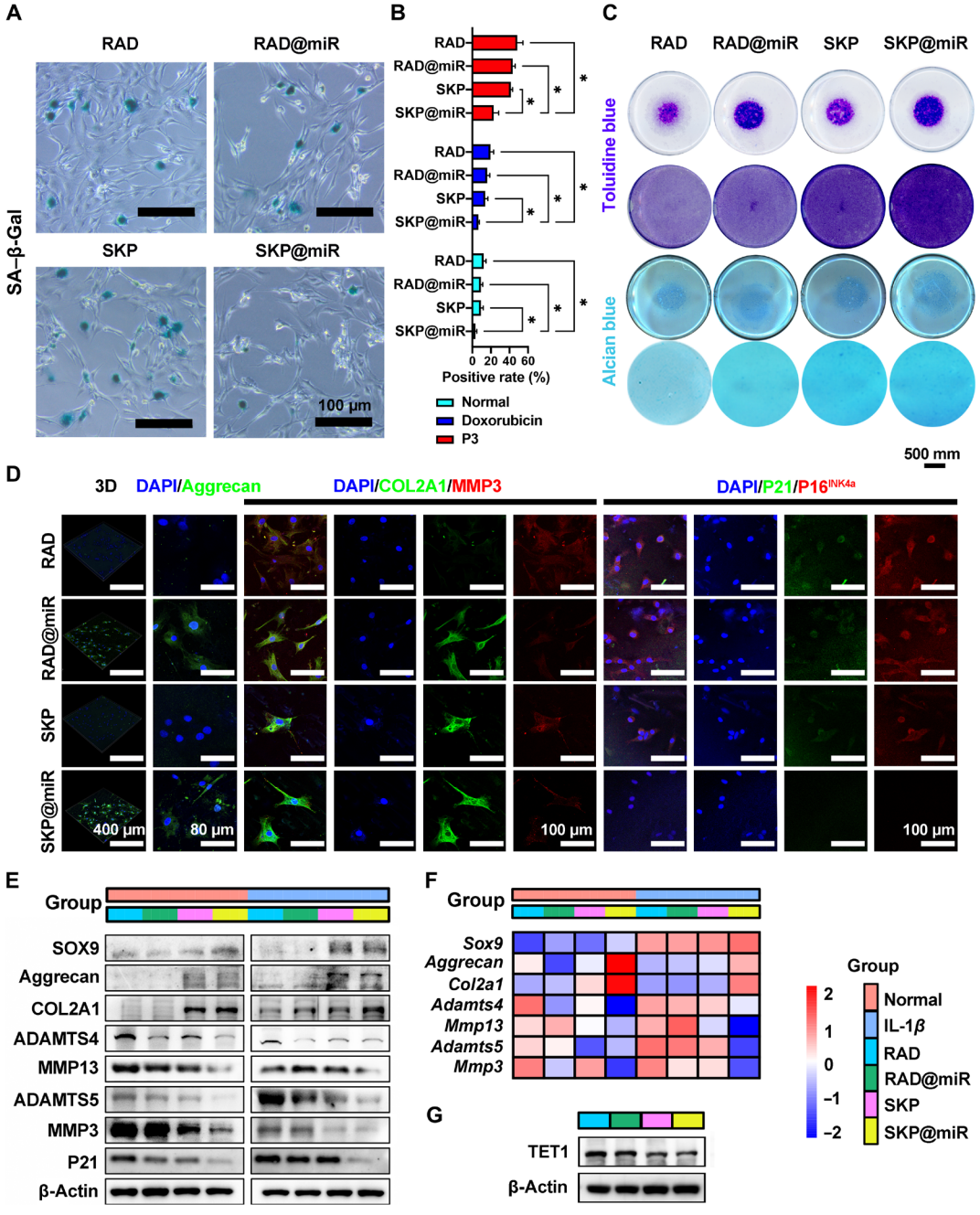

Fig. 6. SKP@miR alleviates senescence and maintains catabolic balance in rat chondrocytes. (**A**) SA–β-Gal staining images of rat chondrocytes cultured on RAD, RAD@miR, SKP, and SKP@miR for 7 days. (**B**) Quantification of SA–β-Gal positivity in normal chondrocytes, doxorubicin-treated chondrocytes, and chondrocytes at passage 3 (P3). $n = 3$. (**C**) Toluidine blue and Alcian blue staining of chondrocyte micromasses and monolayer chondrocytes cultured with hydrogels for 3 days. (**D**) Immunofluorescence staining of aggrecan, COL2A1, MMP3, P21, and $P16^{INK4a}$ of rat chondrocytes cultured on hydrogels for 7 days. (**E**) WB analysis of protein levels of SOX9, aggrecan, COL2A1, ADAMTS4, MMP13, ADAMTS5, MMP3, and P21 in normal and IL-1β–treated chondrocytes cultured on hydrogels for 7 days. (**F**) qRT-PCR analysis of gene expression of *Sox9*, *Aggrecan*, *Col2a1*, *Adamts4*, *Mmp13*, *Adamts5*, and *Mmp3* in normal chondrocytes and IL-1β–treated chondrocytes cultured on hydrogels for 7 days. IL-1β treatment was performed every 2 days. (**G**) WB analysis of TET1 in normal chondrocytes cultured on hydrogels for 7 days. Data are presented as means ± SD. Statistical analysis was performed using one-way ANOVA. *$P < 0.05$.

SMSCs were densely packed at the synovium and distributed in clumps or sheets around the articular surface in the groups with SKP (Fig. 7B and fig. S8). In addition, the SMSCs could be found to infiltrate into the surface of cartilage, suggesting a possibility to differentiate to chondrocytes. Consistently, the Transwell assay revealed that a significantly larger number of cells cultured with SKP and SKP@miR had migrated to the lower side of the porous membrane compared to those cultured with RAD and RAD@miR (Fig. 7, C and D). Moreover, the SKP@miR could enhance the proliferation, cell viability, and adhesion of SMSCs, reflecting the

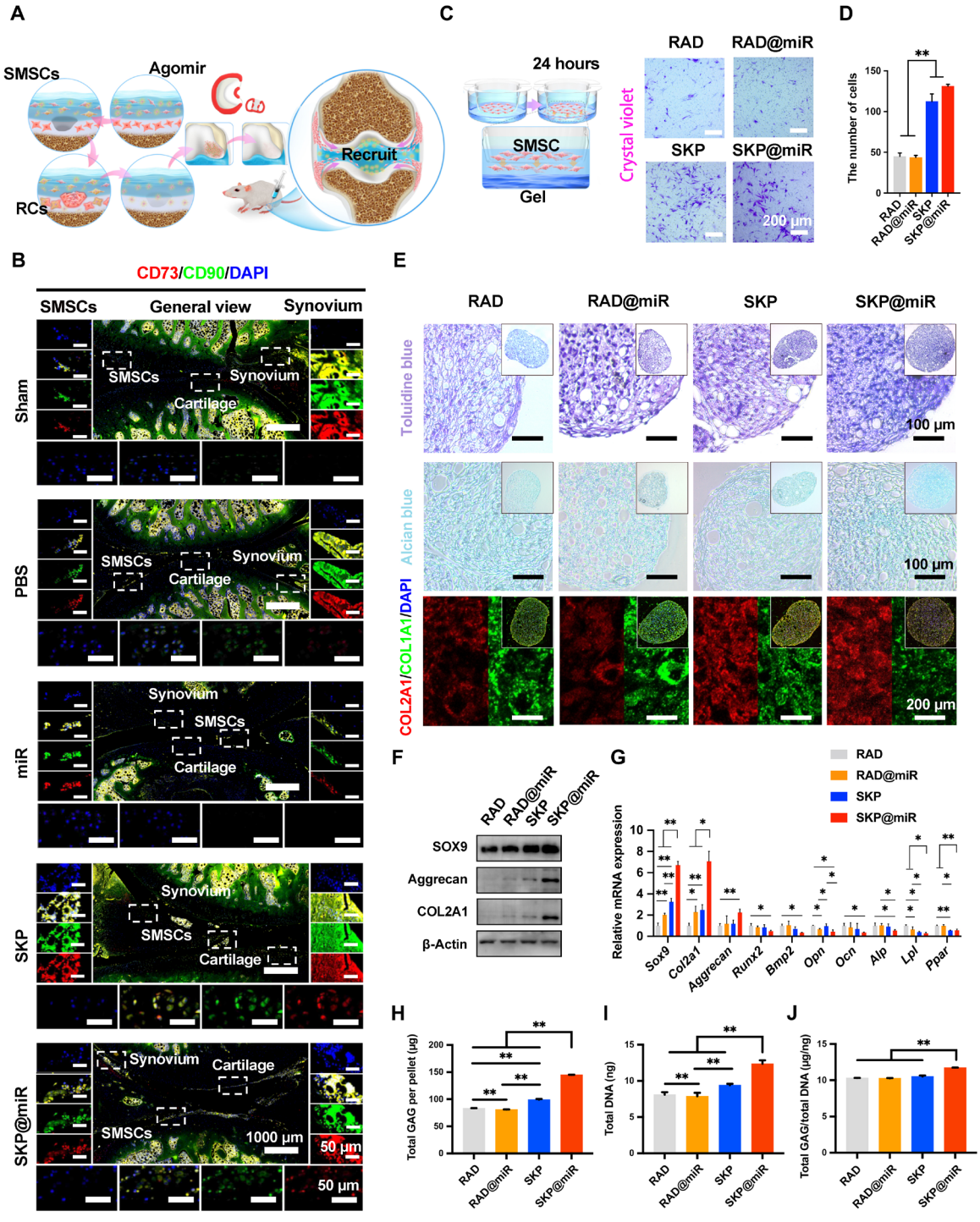

Fig. 7. SKP@miR induces SMSC recruitment and promotes chondrogenic differentiation. (**A**) Schematic illustration of the recruitment process pattern of SMSCs during cartilage repair. (**B**) Immunofluorescence staining of CD90 and CD73 in rat knee joints at 7 weeks after ACLT surgery. SMSCs (left), synovium (right), and chondrocytes (bottom) were shown. Nuclei were stained with DAPI. $n = 4$ rats per group. (**C**) Schematic illustration of Transwell assay to monitor SMSC recruitment in vitro. Representative images of Transwell bottom membrane stained with crystal violet after 24-hour culture. (**D**) Quantification of cells observed at the bottom of the membrane. $n = 3$. (**E**) Toluidine blue staining, Alcian blue staining, and immunofluorescence staining of COL2A1 and COL1A1 in SMSC pellets after 14-day culture on RAD, RAD@miR, SKP, and SKP@miR. (**F**) WB analysis of protein levels of SOX9, aggrecan, and COL2A1 in SMSC pellets. (**G**) qRT-PCR analysis of gene expression of *Sox9*, *Col2a1*, *Aggrecan*, *Runx2*, *Bmp2*, *Opn*, *Ocn*, *Alp*, *Lpl*, and *Ppar* in SMSC pellets. $n = 3$. Values were normalized to β-actin levels, and RAD group was used as the control group. (**H** to **J**) Quantification of total GAG content per pellet (H), total DNA content per pellet (I), and GAG/DNA content (J) of SMSC pellets. Data are presented as means ± SD. Statistical analysis was performed using one-way ANOVA. $^{*}P < 0.05$ and $^{**}P < 0.01$.

satisfactory ability to maintain stem cell population and vitality (fig. S9, A and B). On the basis of the observation of stem cell infiltration in vivo, we evaluated the effect of SKP@miR on the chondrogenic differentiation of SMSCs. The SMSC pellets were cultured with different hydrogels for 14 days with the supplementation of transforming growth factor–β (TGF-β) in culture medium. All the pellets were positive for toluidine blue staining, Alcian blue staining, and COL2A1 staining, while those on SKP@miR exhibited enhanced glycosaminoglycan (GAG) synthesis and COL2 expression (Fig. 7E). The protein levels of SOX9, COL2A1, and aggrecan in SKP@miR group were higher than those in other groups at 14 days (Fig. 7F). SMSC pellets on SKP@miR exhibited significantly up-regulated expression of *Sox9* and *Col2a1* compared with those on RAD, RAD@miR, and SKP and significantly up-regulated *Aggrecan* compared with those on RAD, which was consistent with the WB results (Fig. 7G). The expression of *Runx2*, *Bmp2*, *Lpl*, *Ppar*, *Ocn*, *Opn*, and *Alp* was down-regulated in the SKP@miR group, indicating that the osteogenic or adipogenic differentiation was inhibited by the hydrogel. Besides, the differentiated SMSC pallets cultured with SKP@miR had significantly higher overall GAG content and GAG normalized to DNA than those cultured with other hydrogels (Fig. 7, H to J). These results indicated that the SKP@miR could enhance the chondrogenic differentiation of SMSCs.

To obtain insight into the mechanism by which SKP@miR acts on SMSCs, we performed mRNA sequencing analysis of SMSCs cultivated on different substrates without differentiation-inducing medium for 7 days. Considering the two components in SKP@miR, the individual role of miR-29b-5p and stem cell–homing hydrogel were evaluated and analyzed to demonstrate their synergistic effect on cell behavior. Compared with the control group, a total of 14,378 differentially expressed genes (DEGs) were identified among miR, SKP, and SKP@miR groups, of which 10,400 were up-regulated and 3978 were down-regulated [$P < 0.05$, $|\log_2(\text{fold change})| > 1$]. SKP@miR was found to be largely functional, with 7576 DEGs, followed by SKP, with 6740 DEGs, and lastly, miR, with 62 DEGs (Fig. 8A). In addition, 6375 of DEGs existed both in SKP and SKP@miR groups, while 1192 of DEGs were unique in SKP@miR group, indicating that SKP peptide and miR-29b-5p act synergistically. The gene ontology (GO) analysis among the four groups implied a strong correlation of DEGs with cell differentiation, cell adhesion, cell proliferation, and cell migration (Fig. 8B). Kyoto Encyclopedia of Genes and Genomes (KEGG) enrichment bar plot demonstrated functions related to cell motility, replication and repair, and aging (Fig. 8C). KEGG pathway analysis among RAD, RAD@miR, SKP, and SKP@miR groups indicated that DEGs were also enriched for functional annotations relating to cell adhesion and growth, as well as cellular senescence, TGF-β signaling pathway, and signaling pathways regulating pluripotency of stem cells, which were involved in cartilage repair and the suppression of senescence (Fig. 8D). The gene set enrichment analysis (GSEA) results also showed that the function of SKP was enhanced with the addition of agomir-29b-5p (Fig. 8E). Cell adhesion, cell migration, cell differentiation, and extracellular space/region played major roles in the comparison of RAD and SKP (fig. S9, C and D). Cartilage development was found to be important when comparing RAD with RAD@miR (fig. S9, E and F). Next, the cell adhesion, migration, and senescence functions were analyzed emphatically, and down-regulated expression in adhesion/senescence-associated genes and up-regulated expression in migration-related genes were found in SKP and SKP@miR (Fig. 8F). The expression of key genes associated with cell migration, including *Mmp9*, *Mif*, *Agt*, *Hspb1*, and *Bax*, was evaluated. Compared with RAD and RAD@miR, SKP and SKP@miR exhibited obvious migration effect on SMSCs. The key genes of cell adhesion were also assessed, among which most genes were down-regulated in the SKP and SKP@miR groups compared with those in RAD and RAD@miR groups. The expression of most genes related to cartilage development was up-regulated in RAD@miR and SKP@miR groups, while the expression of cellular senescence-associated genes was significantly down-regulated in SKP@miR group, indicating that SKP and agomirs had synergistic effects on promoting cartilage development and suppressing cellular senescence (Fig. 8G). In addition, genes that related to four basic functions, including cellular senescence, focal adhesion, cartilage development, and cell migration, were subjected to the intersection analysis, indicating some intersection among the functions (Fig. 8H). Collectively, our results demonstrated that SKP@miR could improve the proliferation and migration of SMSCs and induce their differentiation toward chondrocytes, contributing to the regeneration of cartilage defects caused by OA.

DISCUSSION

Current treatments for OA, such as physiotherapy, medications, and surgery, fail to achieve satisfactory therapeutic effects because they only promote symptomatic relief without slowing or stopping the biological process underlying tissue damage (*40*–*42*). Recently, mounting evidence suggests that aging contributes to OA development. The progressive cartilage breakdown in OA joints, the major therapeutic target, is mainly caused by the activation of matrix-degrading enzymes and the limited regeneration capacity of chondrocytes, both of which are closely associated with chondrocyte senescence, one of the hallmarks of aging. Selective elimination of senescent cells effectively prevents OA development by eradicating the source of the catabolic mediators (*43*, *44*), which, however, could cause an excessive reduction in sparser chondrocytes in human cartilage and accelerate the exhaustion of stem cells (*45*, *46*). Besides, the potential off-target effects of senolysis could affect beneficial cells (*4*). More effective strategies, including gene therapy and stem cell therapy, to suppress senescence and improve repair capacity in OA joints have been verified to be profitable to OA treatment.

Recently, RNA interference exhibited the ability to alleviate chondrocyte senescence during OA progression. Here, we proposed a strategy to suppress senescence through long-term and stable delivery of a senescence-associated miRNA, miR-29b-5p, using a stem cell–homing hydrogel to ameliorate cartilage degeneration in OA. In this strategy, the regulation of senescence genes and expansion of chondrocyte pools are combined to attain a synergistic effect on fundamentally settling OA-induced cartilage breakdown. Extended and effective treatments have been achieved by modulating the physiological processes of the organism itself to effectively promote cartilage regeneration and alleviate the aging of the joint, which has not been reported previously. On the one hand, the sustained release of miR-29b-5p from SKP@miR protects the joints by inhibiting chondrocyte senescence, thereby attenuating the imbalance between matrix catabolism and anabolism, representing an alternative strategy to avoid the excessive or unintended removal of cell populations from the damaged cartilage caused by senolytic therapy (Figs. 5 and 6). On the other hand, the SKPPGTSS peptide in SKP@miR expands the quantity of new chondrocytes by recruiting endogenous SMSCs and inducing chondrogenic differentiation, which further contributes to

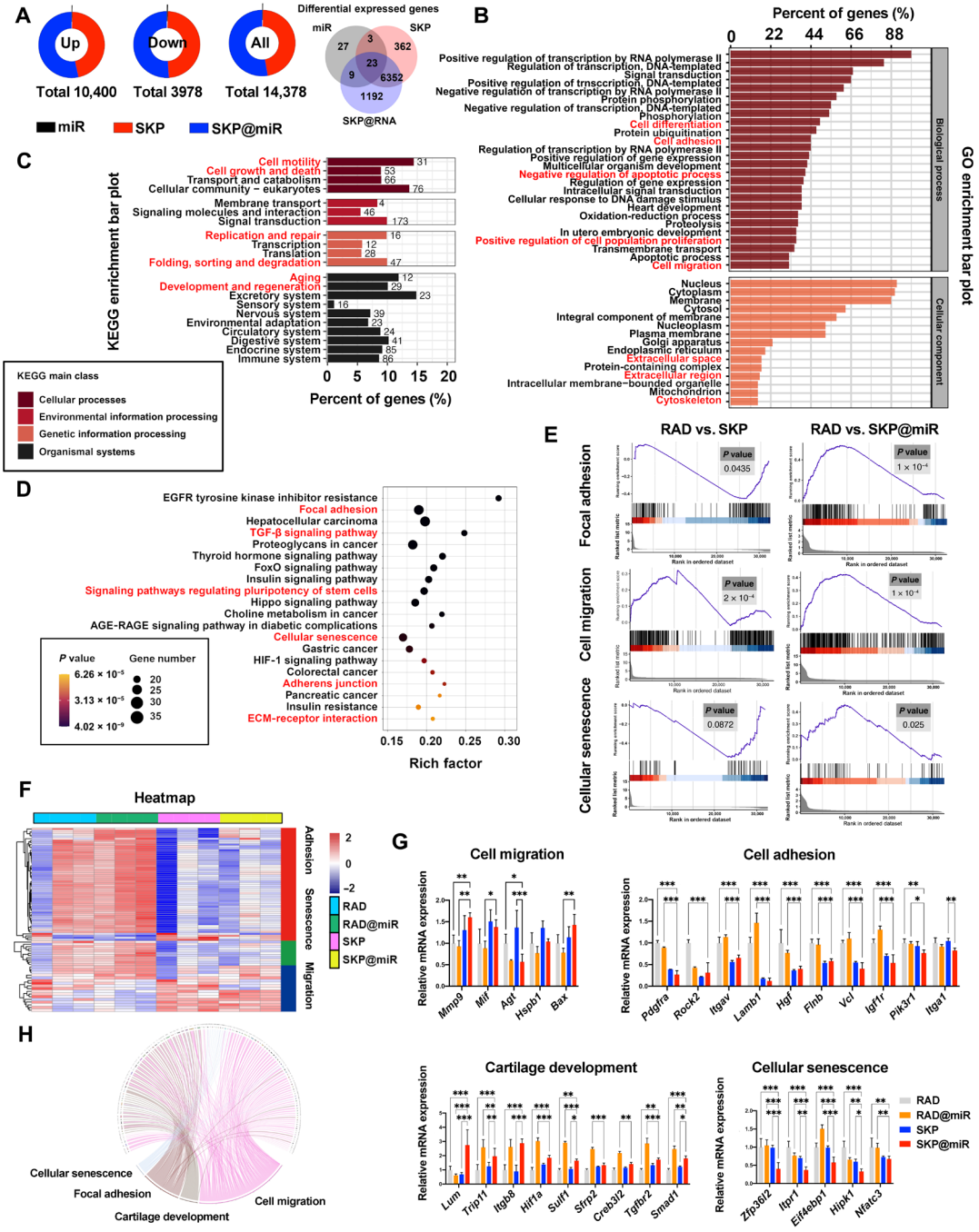

Fig. 8. Intrinsic mechanisms of SKP@miR on SMSC behavior. (**A**) Differentially expressed mRNA in miR, SKP, and SKP@miR groups [$^*P < 0.05$, $|\log_2(\text{fold change})| > 1$]. (**B**) GO enrichment bar plots (cell differentiation, cell adhesion, negative regulation apoptotic process, positive regulation of cell population proliferation, and cell migration). (**C**) KEGG enrichment bar plots (cell motility, cell growth and death, replication and repair, folding, sorting and degradation, aging, and development and regeneration). (**D**) KEGG enrichment analysis (focal adhesion, TGF-β signaling pathway, signaling pathways regulating pluripotency of stem cells, cellular senescence, adherens junction, and ECM-receptor interaction). AGE-RAGE, age range; HIF-1, hypoxia inducible factor-1. (**E**) GSEA enrichment analysis of focal adhesion between RAD and SKP ($P = 0.0435$) and between RAD and SKP@miR ($P < 0.0001$), cellular senescence between RAD and SKP ($P = 0.0872$) and between RAD and SKP@miR ($P = 0.025$), and cell migration between RAD and SKP ($P < 0.0002$) and between RAD and SKP@miR ($P < 0.0001$). (**F**) Heatmap of genes related to cell adhesion, senescence, and migration in RAD, RAD@miR, SKP, and SKP@miR groups. $n = 3$. (**G**) qRT-PCR analysis of genes associated with cell migration, cell adhesion, cartilage development, and cellular senescence. $n = 3$. (**H**) Expression and crossover of each gene of cellular senescence, focal adhesion, cartilage development, and cell migration. Data are presented as means ± SD. Statistical analysis was performed using one-way ANOVA. $^*P < 0.05$, $^{**}P < 0.01$, and $^{***}P < 0.001$.

rejuvenating the aging joint (Figs. 7 and 8). After being treated with SKP@miR, the knee joints with OA after ACLT surgery recover to a comparable level to normal joints, with decreased defects and synovitis, maintained cartilage integrity, and little cartilage degeneration (Fig. 4). Therefore, this strategy and the SKP@miR suggest a promising therapeutic treatment for OA.

The miR-29b-5p has been verified to play an important role in cancer, multiple sclerosis, and other diseases, but there are no reports for the function of miR-29b-5p in OA (*47*). We identified that miR-29b-5p was closely related to both OA and chondrocyte senescence. miRNAs are superior in modulating multiple cellular pathways simultaneously, which is difficult to target by small molecules and therapeutic proteins. One plausible mechanism underlying the therapeutic action of miR-29b-5p involves cartilage protection by silencing various genes, such as *TET1*, and multiple pathways that are crucial in OA or senescence pathogenesis, such as Rap1, phosphatidylinositol 3-kinase–Akt, and mitogen-activated protein kinase signaling pathways (*48*, *49*). Particularly, methylcytosine dioxygenase TET1, a hydroxymethylase predominantly responsible for the accumulation of pathogenic 5-hydroxymethylcytosine in OA, is a direct target of miR-29b-5p. The loss of TET1 impairs both OA initiation and progression, and the siRNA-mediated silencing of TET1 decreased MMP3 and MMP13 expression, which is consistent with our results (*35*). Thus, miR-29b-5p is an effective intervention for OA by modulating TET1 activity and consequent changes in gene transcription.

The effective delivery of miRNAs to the desired site is necessary to achieve therapeutic efficacy. Compared with widely used traditional nanoparticle-based delivery approaches, hydrogels offer water-swollen networks with biodegradability and injectability, overcoming many concerns for drug delivery such as undesirable off-target cytotoxicity and accumulation. The long-term bioactivity and sustained release of agomir-29b-5p were maintained by the hydrogel-based delivery system, contributing to the effective treatment of chronic diseases such as OA and solving the problem of the repeated dosing of miR-29b-5p oligonucleotides due to their low stability (*50*). Compared with the single intra-articular injection of miR-29b-5p, which was ineffective in preventing OA progression, SKP@miR considerably improved the deformation, senescence, and viability of extant cartilage throughout the joint after 10 weeks. The agomirs are concentrated and eluted locally, which decreases the concentrations required for therapeutic efficacy. The release rate of agomirs from hydrogels is directly affected by electrostatic properties because of the anionic charge of nucleic acids. For instance, hydrogels from cationic polymers including polyethylenimine, chitosan, and polyamidoamine contribute to enhanced bioactivity and transfection of miRNA (*51*). The agomir-29b-5p was retained in SKP@miR via electrostatic interaction with cationic lysine and underwent sustained release for 40 days in vitro, which was much longer than that observed with RAD@miR and other hydrogels such as alginate and collagen hydrogels (*52*). Besides, the cholesterol in agomirs tends to aggregate with itself because of hydrophobicity, causing entrapment within the network formed by nanofibers of SAPs, further extending the release period (*53*). The released agomir-29b-5p from SKP@miR maintained good penetration capacity comparable to free agomirs in vivo. However, cationic polymers with positive charges are considered to have cytotoxicity for inducing formation of defects in cellular membrane. Chondrocytes and SMSCs on SKP@miR exhibited healthy morphology and good proliferation, suggesting no cytotoxicity. Inevitably, the movement of the joints may pulverize the injected hydrogel, leading to a more rapid release of agomir-29b-5p in vivo than that in vitro. Nevertheless, the dynamic interactions between SKP peptide and agomir-29b-5p might protect agomir-29b-5p from degradation even in a separated hydrogel.

The SKP@miR hydrogel-based delivery system not only provides the sustained release of agomir-29b-5p but also offers suitable microenvironment in situ because of its injectability, allowing the controlled and minimally invasive delivery of gene vectors in a spatiotemporally precise manner and reduces intra-articular vector spread and possible loss of the therapeutic gene product (*54*). The hydrogel is highly hydrophilic and favorable for lubrication, effectively avoiding the direct collisions between joints, which could provide a protection for the nearby cartilage to some extent. The functionalized hydrogel has the potential to recruit endogenous SMSCs and induce the chondrogenic differentiation in vivo. Considering the limited proliferation and regenerative capacity of senescent chondrocytes in OA, articular cartilage loss is difficult to restore. Exogenous MSCs are excellent alternative cell sources to chondrocytes for cartilage regeneration (*55*). However, their applications are hampered by ethical concerns and low yield of target cells. Not only culture-expanded MSCs but also native joint-resident MSCs play important roles in repairing joint damage in OA (*56*). Although bone MSCs (BMSCs) are widely used in cartilage repair, native BMSCs in OA are rare (*57*). Local expansion of BMSCs was triggered by stimulating a regenerative response via MF surgery (*58*). However, the fibrocartilage formed after MF substantially affected the intrinsic mechanical properties (*59*). Joint-resident MSCs, including synovium-resident and synovial fluid–resident MSCs, contribute to the maintenance and repair of superficial injuries caused by OA and can directly migrate from the synovium and synovial fluid to the sites of injuries (*60*). Endogenous synovial fluid MSCs are capable of adhering to cartilage in a favorable biochemical and biomechanical environment in OA joints. Nevertheless, synovial fluid–resident MSCs are very rarely found in the OA synovial fluid, thus limiting their therapeutic effects. On the contrary, the synovium is a rich source of chondrogenic MSCs (~1%), and previous studies have suggested that synovial fluid–resident MSCs originate from the synovium (*61*). In addition, the synovium and cartilage originate from a common pool of cells during the development of synovial joints, suggesting that SMSCs are the most closely related to chondrocytes developmentally (*62*). Previous studies demonstrated that tissue engineered constructs derived from synovial MSCs combined with nanofibrous scaffolds could repair meniscal hoop structure and prevent the progression of cartilage degeneration. Rabbit synovial fluid MSCs were directly injected or encapsulated in an injectable hydrogel to repair cartilage defects, but few studies have reported the application of SMSCs in cartilage repair, especially endogenous SMSCs. Compared with other study, where postoperative intra-articular injected SMSCs were recruited by SDF-1α (stromal cell-derived factor-1 alpha)–binding decellularized fibrocartilage matrix to repair rotator cuff (*63*), we used a stem cell–homing peptide to recruit the endogenous SMSCs and stimulate regenerative process in cartilage, reducing the risk of using exogenous cells. We speculate that the BMHP SKP contributed to the migration of SMSCs and/or the homing of SMSCs near the cartilage surface. In our previous work, similar stem cell recruitment was observed in which SKP promoted the recruitment of BMSCs toward the defect site filled with SKP-modified scaffold (*23*). Besides, the in vitro Transwell evaluation also confirmed that SKP could promote the migration of SMSCs. Above all, we think that SKP is highly

likely to have a positive effect on the migration and recruitment of SMSCs. However, the mechanism needs to be further investigated. Furthermore, it is recently found that cartilage-derived stem/progenitor cells (CSPCs) residing in the superficial zone of articular cartilage have shown great potential for cartilage repair and OA treatment by adjusting ECM remodeling in early OA (*64*). Our results indicated that agomirs delivered by hydrogels could penetrate into the surface of cartilage, which might also have an effect on the local CSPCs and promote ECM reconstruction. However, more investigations are needed to demonstrate the role of CSPCs. The chondrogenic differentiation of SMSCs was also enhanced by SKP@miR, as evidenced by the up-regulated expression of *Col2a1* and *Aggrecan*. The effects of SKP@miR on SMSCs were further confirmed by the transcriptome analysis. In line with our hypothesis and observation, numerous DEGs are associated with cell adhesion, migration, and differentiation. In addition, GO and KEGG results reveal a potential effect on cellular senescence, which might attribute to miR-29b-5p. The integration of SKP and agomir-29b-5p leads to notably higher expression of these migration-associated and regeneration-associated genes and an expanded quantity of DEGs compared with that of individuals, suggesting a synergistic effect. However, some of the migration-associated genes are down-regulated in SKP@miR after 7 days, probably because of the almost finished migration induced in the early stage, which requires further study to confirm. These findings are of great significance to help explain the mechanism of hydrogel-induced behavior of endogenous SMSCs in vivo.

The regeneration of cartilage damage in OA prompts that a synergistic effect of miR-29b-5p and recruited SMSCs would contribute to delaying and terminating the progression of OA, which is suggested at the cellular and genetic levels in this study. Not only the inhibition of chondrocyte senescence but also the recruitment and differentiation of SMSCs were enhanced in the presence of both agomir-29b-5p and SKP hydrogel. In addition, the cartilage morphology in joints injected with SKP@miR exhibited the best recovery. Here, the synergistic effect lies in two ways. For one, the influence of miR-29b-5p and SKP hydrogel is complementary to each other. Cell cycle arrest caused by accumulated DNA damage and strong growth signal from damaged cartilage together contribute to the chondrocyte senescence and imbalanced metabolism, thus resulting in constant aggravation of cartilage degeneration (*65*). The miR-29b-5p could restore the changed gene pattern caused by DNA damage to a certain extent and down-regulated the $P16^{INK4a}$, P21, and MMPs to inhibit the matrix catabolism and further cartilage damage. The recruited SMSCs by SKP hydrogel could supplement the lost aging chondrocytes and repair the cartilage damage, which decreased the growth signal and then inhibited a series of changes induced by further senescence. Without the supplement of new chondrocytes from SMSCs, the strong growth signal from damaged cartilage would probably induce successive senescence. While without miR-29b-5p, the imbalance of metabolism would not be inhibited to stop the cartilage damage. For another, the combination of miR-29b-5p and SKP hydrogel resulted in more genetic regulations than individuals. The gene expression related to cellular senescence, adhesion, migration, and cartilage development was markedly changed because of SKP@miR, which was consistent with the in vitro and in vivo results. Other studies associated with gene therapy and stem cell therapy to treat OA only demonstrated the individual effect (*66*, *67*). However, few studies take the advantages of this synergistic mechanism to design strategies for OA treating. Therefore, our strategy offers an effective treatment by the synergistic combination of miR-29b-5p and SKP hydrogel.

In summary, we report a stem cell–homing hydrogel-based miRNA delivery system as a disease-modifying agent for OA by suppressing senescence to prevent cartilage degeneration and promote matrix regeneration. miR-29b-5p can effectively alleviate the current state of existing articular cartilage and delay the progression of aging to prevent the rapid progression of OA. SKP@miR attenuates the imbalance between matrix synthesis and inflammatory phenotypes in senescent chondrocytes and OA joints. In addition, the hydrogel recruits SMSCs and induces differentiation toward chondrocytes to repair the defects and form new cartilage without using exogenous stem cells. The OA joints treated with SKP@miR exhibit improved cartilage similar to normal cartilage. Future directions include optimization of the hydrogel formulation to achieve better therapeutic effects in large-animal models before its translation in the clinical practice and exploration on its effectiveness in patients whose OA is driven by other mechanisms, such as obesity or genetic factors. Collectively, the injectable cell-free and off-the-shelf approach is more convenient and practical for clinical applications, which will shed light on developing disease-modifying therapies that benefit patients with OA.

MATERIALS AND METHODS

Study design

We aimed to develop a therapeutic approach for attenuating cartilage degeneration and rejuvenating cartilage breakdown during OA by delivering miR-29b-5p from an injectable stem cell–homing hydrogel. We first screened miR-29b-5p whose up-regulation could effectively modulate the senescent and OA phenotypes of chondrocytes and investigated their regulatory effects in rat and human chondrocytes. The in vivo effects of agomir-29b-5p were evaluated in aging mouse models. Moreover, the underlying mechanisms and downstream target TET1 of miR-29b-5p were identified and verified in rat chondrocytes. The functional peptide motif SKPPGTSS mimicking the bioactivity of BMHP was incorporated into the SAP RAD for the recruitment of endogenous SMSCs. SKP@miR was prepared by combining agomir-29b-5p and functionalized SAPs and was characterized using CD (circular dichroism), FTIR, atomic force microscopy, scanning electron microscopy, transmission electron microscopy, and rheology analysis. The interaction between agomirs and peptides was evaluated via molecular docking. The release of agomirs from SKP@miR was assessed both in vitro and in vivo, with RAD, RAD@miR, and SKP as the control groups. The penetration capacity of agomirs in hydrogels was evaluated using porcine cartilage explant penetration assay. We further evaluated the proliferation, adhesion, and morphology of rat chondrocytes and SMSCs on the hydrogels to assess its biocompatibility. We examined the effects of hydrogels on the senescence of rat chondrocytes under inflammatory stimuli. In vitro SMSC recruitment was performed to assess stem cell affinity and migration toward the hydrogels. The differentiation of SMSCs on hydrogels was evaluated after 14 days using the pellet culture assay with chondrogenic differentiation medium. To reveal the mechanism of hydrogel-induced stem cell behavior, we performed RNA sequencing analysis of SMSCs cultured on hydrogels for 7 days without using the differentiation medium. ACLT surgery was then used to induce posttraumatic OA in 4-week-old rats. The hydrogels were delivered into rat knee joints by

intra-articular injection at 4 weeks postoperatively. Various OA manifestations, including cartilage destruction, osteophyte maturity, and synovial inflammation were histologically assessed and scored at 7 and 10 weeks postoperatively. Reaction time on hot plates was measured as a behavioral assessment of OA-induced pain. In vivo MSC recruitment was assessed using immunofluorescence staining.

Rats used for animal studies were randomly assigned to each group, and all samples were analyzed by experienced histopathologists who were blinded to the experimental conditions. For each experiment, the sample size reflected the number of independent biological replicates and is indicated in the figure legends. Persistent lameness and discomfort after surgical recovery were used as the criteria for stopping further experiments with the corresponding rat before completion. None of the animals met these criteria. No data were excluded from the analysis. All animal experiments were approved by the laboratory animal management and ethics committee (approval number IACUC-20190715-10) following the Institutional Animal Care and Use Committee (IACUC) guidelines. Additional information related to the experimental procedures can be found in the Supplementary Materials.

Statistical analysis

For hydrogel characterization and in vitro studies, each experiment was conducted independently at least three times. Data are presented as means ± SD and analyzed using two-tailed Student's *t* test or one-way analysis of variance (ANOVA), followed by Tukey's or Dunnett's T3 post hoc tests for multiple comparisons. Statistical analysis was performed using Prism GraphPad 8.0 software. $P < 0.05$ was considered statistically significant.

SUPPLEMENTARY MATERIALS

Supplementary material for this article is available at https://science.org/doi/10.1126/sciadv.abk0011

View/request a protocol for this paper from *Bio-protocol*.

REFERENCES AND NOTES

1. J. M. Hootman, C. G. Helmick, Projections of US prevalence of arthritis and associated activity limitations. *Arthritis Rheum.* **54**, 226–229 (2006).
2. R. F. Loeser, S. R. Goldring, C. R. Scanzello, M. B. Goldring, Osteoarthritis: A disease of the joint as an organ. *Arthritis Rheum.* **64**, 1697–1707 (2012).
3. D. J. Hunter, S. Bierma-Zeinstra, Osteoarthritis. *Lancet* **393**, 1745–1759 (2019).
4. D. Prieto-Alhambra, A. Judge, M. K. Javaid, C. Cooper, A. Diez-Perez, N. K. Arden, Incidence and risk factors for clinically diagnosed knee, hip and hand osteoarthritis: Influences of age, gender and osteoarthritis affecting other joints. *Ann. Rheum. Dis.* **73**, 1659–1664 (2014).
5. H. Stanton, F. M. Rogerson, C. J. East, S. B. Golub, K. E. Lawlor, C. T. Meeker, C. B. Little, K. Last, P. J. Farmer, I. K. Campbell, A. M. Fourie, A. J. Fosang, ADAMTS5 is the major aggrecanase in mouse cartilage in vivo and in vitro. *Nature* **434**, 648–652 (2005).
6. C. Amor, J. Feucht, J. Leibold, Y.-J. Ho, C. Y. Zhu, D. Alonso-Curbelo, J. Mansilla-Soto, J. A. Boyer, X. Li, T. Giavridis, A. Kulick, S. Houlihan, E. Peerschke, S. L. Friedman, V. Ponomarev, A. Piersigilli, M. Sadelain, S. W. Lowe, Senolytic CAR T cells reverse senescence-associated pathologies. *Nature* **583**, 127–132 (2020).
7. B. A. Lakin, B. D. Snyder, M. W. Grinstaff, Assessing cartilage biomechanical properties: Techniques for evaluating the functional performance of cartilage in health and disease. *Annu. Rev. Biomed. Eng.* **19**, 27–55 (2017).
8. B. G. Childs, M. Durik, D. J. Baker, J. M. van Deursen, Cellular senescence in aging and age-related disease: From mechanisms to therapy. *Nat. Med.* **21**, 1424–1435 (2015).
9. D. P. Bartel, MicroRNAs: Target recognition and regulatory functions. *Cell* **136**, 215–233 (2009).
10. R. Vicente, D. Noel, Y. M. Pers, F. Apparailly, C. Jorgensen, Deregulation and therapeutic potential of microRNAs in arthritic diseases. *Nat. Rev. Rheumatol.* **12**, 211–220 (2016).
11. C. Zhao, Y. Miao, Z. Cao, J. Shi, J. Li, F. Kang, C. Dou, Z. Xie, Q. Xiang, S. Dong, MicroRNA-29b regulates hypertrophy of murine mesenchymal stem cells induced toward chondrogenesis. *J. Cell. Biochem.* **5**, 8742–8753 (2019).
12. D. Moulin, V. Salone, M. Koufany, T. Clement, I. Behm-Ansmant, C. Branlant, B. Charpentier, J.-Y. Jouzeau, MicroRNA-29b contributes to collagens imbalance in human osteoarthritic and dedifferentiated articular chondrocytes. *Biomed. Res. Int.* **2017**, 9792512 (2017).
13. U. Mayer, A. Benditz, S. Grässel, miR-29b regulates expression of collagens I and III in chondrogenically differentiating BMSC in an osteoarthritic environment. *Sci. Rep.* **7**, 13297 (2017).
14. J. Du, M. Li, Q. Huang, W. Liu, W. Q. Li, Y. J. Li, Z. C. Gong, The critical role of microRNAs in stress response: Therapeutic prospect and limitation. *Pharmacol. Res.* **142**, 294–302 (2019).
15. E. Herrera-Carrillo, Y. P. Liu, B. Berkhout, Improving miRNA delivery by optimizing mirna expression cassettes in diverse virus vectors. *Hum. Gene Ther. Methods* **28**, 177–190 (2017).
16. J. Conde, N. Oliva, M. Atilano, H. S. Song, N. Artzi, Self-assembled RNA-triple-helix hydrogel scaffold for microRNA modulation in the tumour microenvironment. *Nat. Mater.* **15**, 353–363 (2016).
17. R. Reshke, J. A. Taylor, A. Savard, H. S. Guo, L. H. Rhym, P. S. Kowalski, M. T. Trung, C. Campbell, W. Little, D. G. Anderson, D. Gibbings, Reduction of the therapeutic dose of silencing RNA by packaging it in extracellular vesicles via a pre-microRNA backbone. *Nat. Biomed. Eng.* **4**, 52–68 (2020).
18. M. L. Bobbin, J. J. Rossi, RNA interference (RNAi)-based therapeutics: Delivering on the promise? *Annu. Rev. Pharmacol. Toxicol.* **56**, 103–122 (2016).
19. W. Chen, H. Chen, D. Zheng, H. Zhang, L. Deng, W. Cui, Y. Zhang, H. A. Santos, H. Shen, Gene-hydrogel microenvironment regulates extracellular matrix metabolism balance in nucleus pulposus. *Adv. Sci.* **7**, 1902099 (2020).
20. N. Li, J. Gao, L. Mi, G. Zhang, L. Zhang, N. Zhang, R. Huo, J. Hu, K. Xu, Synovial membrane mesenchymal stem cells: past life, current situation, and application in bone and joint diseases. *Stem Cell Res Ther* **11**, 381 (2020).
21. E. Kozhemyakina, M. J. Zhang, A. Ionescu, U. M. Ayturk, N. Ono, A. Kobayashi, H. Kronenberg, M. L. Warman, A. B. Lassar, Identification of a *Prg4*-expressing articular cartilage progenitor cell population in mice. *Arthritis Rheumatol.* **67**, 1261–1273 (2015).
22. X. Liu, X. Wang, X. Wang, H. Ren, J. He, L. Qiao, F.-Z. Cui, Functionalized self-assembling peptide nanofiber hydrogels mimic stem cell niche to control human adipose stem cell behavior in vitro. *Acta Biomater.* **9**, 6798–6805 (2013).
23. X. Sun, H. Yin, Y. Wang, J. J. Lu, X. Z. Shen, C. F. Lu, H. Tang, H. Y. Meng, S. H. Yang, W. Yu, Y. Zhu, Q. Y. Guo, A. Y. Wang, W. J. Xu, S. Y. Liu, S. B. Lu, X. M. Wang, J. Peng, In situ articular cartilage regeneration through endogenous reparative cell homing using a functional bone marrow-specific scaffolding system. *ACS Appl. Mater. Interfaces* **10**, 38715–38728 (2018).
24. T. M. Tamer, Hyaluronan and synovial joint: Function, distribution and healing. *Interdiscip. Toxicol.* **6**, 111–125 (2013).
25. M. D. Krebs, O. Jeon, E. Alsberg, Localized and sustained delivery of silencing RNA from macroscopic biopolymer hydrogels. *J. Am. Chem. Soc.* **131**, 9204–9206 (2009).
26. N. Habibi, N. Kamaly, A. Memic, H. Shafiee, Self-assembled peptide-based nanostructures: Smart nanomaterials toward targeted drug delivery. *Nano Today* **11**, 41–60 (2016).
27. A. L. Sieminski, C. E. Semino, H. Gong, R. D. Kamm, Primary sequence of ionic self-assembling peptide gels affects endothelial cell adhesion and capillary morphogenesis. *J. Biomed. Mater. Res.* **87A**, 494–504 (2008).
28. X. Liu, X. Wang, A. Horii, X. Wang, L. Qiao, S. Zhang, F.-Z. Cui, In vivo studies on angiogenic activity of two designer self-assembling peptide scaffold hydrogels in the chicken embryo chorioallantoic membrane. *Nanoscale* **4**, 2720–2727 (2012).
29. Q. Ni, F. Zhang, Y. Zhang, G. Zhu, Z. Wang, Z. Teng, C. Wang, B. C. Yung, G. Niu, G. Lu, L. Zhang, X. Chen, In situ shRNA synthesis on DNA–Polylactide nanoparticles to treat multidrug resistant breast cancer. *Adv. Mater.* **30**, 1705737–1705747 (2018).
30. D. Kang, J. Shin, Y. Cho, H.-S. Kim, Y.-R. Gu, H. Kim, K. T. You, M. J. Chang, C. B. Chang, S.-B. Kang, J.-S. Kim, V. N. Kim, J.-H. Kim, Stress-activated miR-204 governs senescent phenotypes of chondrocytes to promote osteoarthritis development. *Sci. Transl. Med.* **11**, eaar6659 (2019).
31. S. Shen, Y. Wu, J. Chen, Z. Xie, K. Huang, G. Wang, Y. Yang, W. Ni, Z. Chen, P. Shi, Y. Ma, S. Fan, CircSERPINE2 protects against osteoarthritis by targeting miR-1271 and ETS-related gene. *Ann. Rheum. Dis.* **78**, 826–836 (2019).
32. A. Haseeb, R. Kc, M. Angelozzi, C. De Charleroy, D. Rux, R. J. Tower, L. Yao, R. Pellegrino Da Silva, M. Pacifici, L. Qin, V. Lefebvre, SOX9 keeps growth plates and articular cartilage healthy by inhibiting chondrocyte dedifferentiation/osteoblastic redifferentiation. *Proc. Natl. Acad. Sci. U.S.A.* **118**, e2019152118 (2021).
33. J. M. Stuart, E. Segal, D. Koller, S. K. Kim, A gene-coexpression network for global discovery of conserved genetic modules. *Science* **302**, 249–255 (2003).
34. J. Campisi, F. d'Adda di Fagagnam, Cellular senescence: When bad things happen to good cells. *Nat. Rev. Mol. Cell Biol.* **8**, 729–740 (2007).
35. P. Smeriglio, F. C. Grandi, S. Davala, V. Masarapu, P. F. Indelli, S. B. Goodman, N. Bhutani, Inhibition of TET1 prevents the development of osteoarthritis and reveals the 5hmC landscape that orchestrates pathogenesis. *Sci. Transl. Med.* **12**, eaax2332 (2020).
36. Y. Lu, B. Brommer, X. Tian, A. Krishnan, M. Meer, C. Wang, D. L. Vera, Q. Zeng, D. Yu, M. S. Bonkowski, J.-H. Yang, S. Zhou, E. M. Hoffmann, M. M. Karg, M. B. Schultz, A. E. Kane, N. Davidsohn, E. Korobkina, K. Chwalek, L. A. Rajman, G. M. Church, K. Hochedlinger,

V. N. Gladyshev, S. Horvath, M. E. Levine, M. S. Gregory-Ksander, B. R. Ksander, Z. He, D. A. Sinclair, Reprogramming to recover youthful epigenetic information and restore vision. *Nature* **588**, 124–129 (2020).
37. K. A. Athanasiou, M. P. Rosenwasser, J. A. Buckwalter, T. I. Malinin, V. C. Mow, Interspecies comparisons of in situ intrinsic mechanical properties of distal femoral cartilage. *J. Orthop. Res.* **9**, 330–340 (1991).
38. A. Mathiessen, P. G. Conaghan, Synovitis in osteoarthritis: Current understanding with therapeutic implications. *Arthritis Res. Ther.* **19**, 18 (2017).
39. J. Sellam, F. Berenbaum, The role of synovitis in pathophysiology and clinical symptoms of osteoarthritis. *Nat. Rev. Rheumatol.* **6**, 625–635 (2010).
40. Q. Wang, A. L. Rozelle, C. M. Lepus, C. R. Scanzello, J. J. Song, D. Meegan Larsen, J. F. Crish, G. Bebek, S. Y. Ritter, T. M. Lindstrom, I. Hwang, H. H. Wong, L. Punzi, A. Encarnacion, M. Shamloo, S. B. Goodman, T. Wyss-Coray, S. R. Goldring, N. K. Banda, J. M. Thurman, R. Gobezie, M. K. Crow, V. Michael Holers, D. M. Lee, W. H. Robinson, Identification of a central role for complement in osteoarthritis. *Nat. Med.* **17**, 1674–1679 (2011).
41. J. H. Kim, J. Jeon, M. Shin, Y. Won, M. Lee, J. S. Kwak, G. Lee, J. Rhee, J. H. Ryu, C. H. Chun, J. S. Chun, Regulation of the catabolic cascade in osteoarthritis by the zinc-ZIP8-MTF1 axis. *Cell* **156**, 730–743 (2014).
42. S. Yang, J. Kim, J. H. Ryu, H. Oh, C. H. Chun, B. J. Kim, B. H. Min, J. S. Chun, Hypoxia-inducible factor-2α is a catabolic regulator of osteoarthritic cartilage destruction. *Nat. Med.* **16**, 687–693 (2010).
43. O. H. Jeon, C. Kim, R. M. Laberge, M. Demaria, S. Rathod, A. P. Vasserot, J. W. Chung, D. H. Kim, Y. Poon, N. David, D. J. Baker, J. M. Van Deursen, J. Campisi, J. H. Elisseeff, Local clearance of senescent cells attenuates the development of post-traumatic osteoarthritis and creates a pro-regenerative environment. *Nat. Med.* **23**, 775–781 (2017).
44. M. Yoshioka, R. D. Coutts, D. Amiel, S. A. Hacker, Characterization of a model of osteoarthritis in the rabbit knee. *Osteoarthr. Cartil.* **4**, 87–98 (1996).
45. D. McHugh, J. Gil, Senescence and aging: Causes, consequences, and therapeutic avenues. *J. Cell Biol.* **217**, 65–77 (2018).
46. J. A. Colins, B. O. Diekman, R. F. Loeser, Targeting aging for disease modification in osteoarthritis. *Curr. Opin. Rheumatol.* **30**, 101–107 (2018).
47. X. Jin, Y. Xu, M. Guo, Y. Sun, J. Ding, L. Li, X. Zheng, S. Li, D. Yuan, S. S. Li, hsa_circNFXL1_009 modulates apoptosis, proliferation, migration, and potassium channel activation in pulmonary hypertension. *Mol. Ther. Nucl. Acids* **23**, 1007–1019 (2021).
48. S. F. Song, J. V. Perez, W. Svitko, M. D. Ricketts, E. Dean, D. Schultz, R. Marmorstein, F. B. Johnson, Rap1-mediated nucleosome displacement can regulate gene expression in senescent cells without impacting the pace of senescence. *Aging Cell* **19**, e13061 (2020).
49. P. Li, Y. B. Gan, Y. Xu, L. Song, L. Y. Wang, B. Ouyang, C. M. Zhang, Q. Zhou, The inflammatory cytokine TNF-α promotes the premature senescence of rat nucleus pulposus cells via the PI3K/Akt signaling pathway. *Sci. Rep.* **7**, 42938 (2017).
50. I. M. Verma, Gene Therapy That Works. *Science* **341**, 853–855 (2013).
51. J. S. Vorhies, J. J. Nemunaitis, Synthetic vs. natural/biodegradable polymers for delivery of shRNA-based cancer therapies. *Methods Mol. Biol.* **480**, 11–29 (2009).
52. L. L. Wang, Y. Liu, J. J. Chung, T. Wang, A. C. Gaffey, M. M. Lu, C. A. Cavanaugh, S. Zhou, R. Kanade, P. Atluri, E. E. Morrisey, J. A. Burdick, Sustained miRNA delivery from an injectable hydrogel promotes cardiomyocyte proliferation and functional regeneration after ischaemic injury. *Nat. Biomed. Eng.* **1**, 983–992 (2017).
53. E. Fröhlich, The role of surface charge in cellular uptake and cytotoxicity of medical nanoparticles. *Int. J. Nanomedicine* **7**, 5577–5591 (2012).
54. H. Madry, L. Gao, A. Rey-Rico, J. K. Venkatesan, K. Muller-Brandt, X. Y. Cai, L. Goebel, G. Schmitt, S. Speicher-Mentges, D. Zurakowski, M. D. Menger, M. W. Laschke, M. Cucchiarini, Thermosensitive hydrogel based on PEO–PPO–PEO poloxamers for a controlled in situ release of recombinant adeno-associated viral vectors for effective gene therapy of cartilage defects. *Adv. Mater.* **32**, 1906508 (2020).
55. Y. B. Park, C. W. Ha, C. H. Lee, Y. C. Yoon, Y. G. Park, Cartilage regeneration in osteoarthritic patients by a composite of allogeneic umbilical cord blood-derived mesenchymal stem cells and hyaluronate hydrogel: Results from a clinical trial for safety and proof-of-concept with 7 years of extended follow-up. *Stem Cells Transl. Med.* **6**, 613–621 (2017).
56. J. R. Steadman, K. K. Briggs, J. J. Rodrigo, M. S. Kocher, T. J. Gill, W. G. Rodkey, Outcomes of microfracture for traumatic chondral defects of the knee: Average 11-year follow-up. *Art Ther.* **19**, 477–484 (2003).
57. D. McGonagle, T. G. Baboolal, E. Jones, Native joint-resident mesenchymal stem cells for cartilage repair in osteoarthritis. *Nat. Rev. Rheumatol.* **13**, 719–730 (2017).
58. M. L. Davies-Tuck, A. E. Wluka, Y. Wang, A. J. Teichtahl, G. Jones, C. Ding, F. M. Cicuttini, The natural history of cartilage defects in people with knee osteoarthritis. *Osteoarthr. Cartil.* **16**, 337–342 (2008).
59. K. Mithoefer, T. Mcadams, R. J. Williams, P. C. Kreuz, B. R. Mandelbaum, Clinical efficacy of the microfracture technique for articular cartilage repair in the knee: An evidence-based systematic analysis. *Am. J. Sports Med.* **10**, 2053–2063 (2009).
60. T. G. Baboolal, S. C. Mastbergen, E. Jones, S. J. Calder, F. P. J. G. Lafeber, D. Mcgonagle, Synovial fluid hyaluronan mediates MSC attachment to cartilage, a potential novel mechanism contributing to cartilage repair in osteoarthritis using knee joint distraction. *Ann. Rheum. Dis.* **75**, 908–915 (2016).
61. I. Sekiya, M. Ojima, S. Suzuki, M. Yamaga, M. Horie, H. Koga, K. Tsuji, K. Miyaguchi, S. Ogishima, H. Tanaka, T. Muneta, Human mesenchymal stem cells in synovial fluid increase in the knee with degenerated cartilage and osteoarthritis. *J. Orthop. Res.* **30**, 943–949 (2012).
62. I. Sekiya, T. Muneta, M. Horie, H. Koga, Arthroscopic transplantation of synovial stem cells improves clinical outcomes in knees with cartilage defects. *Clin. Orthop. Relat. Res.* **473**, 2316–2326 (2015).
63. C. Chen, Y. Chen, M. Li, H. Xiao, Q. Shi, T. Zhang, X. Li, C. Zhao, J. Hu, H. Lu, Functional decellularized fibrocartilaginous matrix graft for rotator cuff enthesis regeneration: A novel technique to avoid in-vitro loading of cells. *Biomaterials* **250**, 119996 (2020).
64. Y. Jiang, R. S. Tuan, Origin and function of cartilage stem/progenitor cells in osteoarthritis. *Nat. Rev. Rheumatol.* **11**, 206–212 (2015).
65. R. F. Loeser, J. A. Collins, B. O. Diekman, Ageing and the pathogenesis of osteoarthritis. *Nat. Rev. Rheumatol.* **12**, 412–420 (2016).
66. Y. Zhang, F. Vasheghani, Y. H. Li, M. Blati, K. Simeone, H. Fahmi, B. Lussier, P. Roughley, D. Lagares, J. P. Pelletier, J. Martel-Pelletier, M. Kapoor, Cartilage-specific deletion of mTOR upregulates autophagy and protects mice from osteoarthritis. *Ann. Rheum. Dis.* **74**, 1432–1440 (2015).
67. J. Platas, M. I. Guillen, M. D. Pérez Del Caz, F. Gomar, M. A. Castejon, V. Mirabet, M. J. Alcaraz, Paracrine effects of human adipose-derived mesenchymal stem cells in inflammatory stress-induced senescence features of osteoarthritic chondrocytes. *Aging (Albany NY)* **8**, 1703–1717 (2016).
68. S. Yang, C. Wang, J. Zhu, C. Lu, H. Li, F. Chen, J. Lu, Z. Zhang, X. Yan, H. Zhao, X. Sun, L. Zhao, J. Liang, Y. Wang, J. Peng, X. Wang, Self-assembling peptide hydrogels functionalized with LN- and BDNF- mimicking epitopes synergistically enhance peripheral nerve regeneration. *Theranostics* **10**, 8227–8249 (2020).
69. J. Zhu, S. Yang, K. Cai, S. Wang, Z. Qiu, J. Huang, G. Jiang, X. Wang, X. Fang, Bioactive poly (methyl methacrylate) bone cement for the treatment of osteoporotic vertebral compression fractures. *Theranostics* **10**, 6544–6560 (2020).
70. T. Gronau, K. Krüger, C. Prein, A. Aszodi, I. Gronau, R. V. Iozzo, F. C. Mooren, H. Clausen-Schaumann, J. Bertrand, T. Pap, Forced exercise-induced osteoarthritis is attenuated in mice lacking the small leucine-rich proteoglycan decorin. *Ann. Rheum. Dis.* **76**, 442–449 (2017).
71. T. Hayami, M. Pickarski, Y. Zhuo, G. A. Wesolowski, G. A. Rodan, L. T. Duong, Characterization of articular cartilage and subchondral bone changes in the rat anterior cruciate ligament transection and meniscectomized models of osteoarthritis. *Bone* **38**, 234–243 (2006).

Acknowledgments: We thank J. Huang, T. Huang, and H. Li at Shimadzu (China) Co. Ltd. for the help of technology and equipment of micro-CT. We thank E. Jiang from Rice University for the help of manuscript preparation. We thank J. Zheng from Tsinghua University for the help of manuscript revision. We also thank X. Xu and colleagues from Zhejiang Chinese Medical University Laboratory Animal Research Center for helping with the animal study. **Funding:** This work was supported by National Key R&D Program of China (no. 2020YFC1107600 and 2018YFB0704304), the National Nature Science Fund of China (no. 81871797), the Key Research and Development Plan in Zhejiang Province (no. 2020C03041), and Medical Healthy Scientific Technology Project of Zhejiang Province (no. WKL-ZJ-2006 and WKJ-ZJ-1906). No benefits in any form have been or will be received from a commercial party related directly or indirectly to the subject of this manuscript. **Author contributions:** J.Z., S.Y., X.W., and X.F. conceived the idea and designed the research project. J.Z., S.Y., Y.-Y.H., Z.Z., and W.Y. fabricated the materials and performed the characterization. J.Z. and S.Y. performed the cell studies. J.Z., S.Y., Z.G., K.L., and P.S. performed the animal studies. J.Z. and Y.Q. performed the bioinformatics analysis. J.Z. and S.Y. analyzed the data, prepared the figures, and wrote the manuscript. Y.Q., H.Z., L.Y., S.F., S.S., A.G.M., X.W., and X.F. reviewed and revised the manuscript. All authors approved the submitted vision of the manuscript. **Competing interests:** The authors declare that they have no competing interests. **Data and materials availability:** All data needed to evaluate the conclusions in the paper are present in the paper and/or the Supplementary Materials.

Submitted 17 June 2021
Accepted 7 February 2022
Published 30 March 2022
10.1126/sciadv.abk0011